LIFE CYCLE ASSESSMENT OF A NOVEL BUILDING-INTEGRATED PHOTOVOLTAIC-THERMAL (BIPVT) SYSTEM

Yuda Sun

Advisor: Prof. Nickolas J. Themelis,

Co-advisors: Profs. Huiming Yin (Civil Eng.) and Vasilis Fthenakis (EAEE)

Submitted in partial fulfillment of the requirements for

M.S. degree in Earth Resources Engineering

Department of Earth and Environmental Engineering

Columbia University

January 2014

Research sponsored by the

Earth Engineering Center

Columbia University

Life cycle assessment of a novel building-integrated photovoltaic-thermal (BIPVT) system

EXECUTIVE SUMMARY

This study presents the results of a detailed performance and environmental analysis of a 2.5 kWp innovative Building Integrated Photovoltaic Thermal (BIPVT) system in three locations in the USA (Phoenix, AZ; Duluth, MN; and Albany, NY) on a residential house roof with slope of 6/12. The studied renewable energy system consists of BIPVT panels, a balance of system (BOS) and a power conditioning system (PCS). Life-cycle environmental issues were analyzed using as major indicators like global warming potential (GWP), cumulated energy demand (CED), and energy payback time (EPBT). The results were compared with those of alternative PV systems and energy sources.

The GWP and EPBT of the BIPVT system varies between different locations. The GWP ranged from 18 to 42g CO_2-e/kWh, and the EPBT from 1.5 to 3.5 years. The system performs the best in Phoenix and the least in Albany. The life cycle effect of different solar cell types on the environmental performance is very limited, although the solar cell always contribute the most to energy use and the least to carbon emission. In comparison to other PV systems or energy sources, the combined BIPVT system has great potential for wide use in buildings

Keywords: BIPVT; building Integrated; renewable energy; photovoltaics; solar thermal; LCA, Life Cycle Assessment; GWP; EPBT

Acknowledgements

The author is grateful to his advisor, Prof. Themelis, for providing invaluable assistance and advice during the course of this thesis. I would also like to acknowledge Prof.Huiming Yin and Dr.Fangliang Chen for their work on the excellent BIPVT system and FGM material, and accept me as a project team member. Thanks and love to Liliana Themelis for her support during this long year. My special thanks also to my parents, for their love and support during my studies at Columbia University.

Table of Contents

List of Figures

List of Tables

Nomenclature

AC	Alternating current
Al	Aluminum
a-Si	Amorphous silicon
BIPVT	Building Integrated Photovoltaic Thermal System
BOS	Balance of system
CED	Cumulative Energy Demand
DC	Direct current
EG-Si	Electronic silicon
EPBT	Energy payback time
FGM	Functionally graded material
GHG	Greenhouse gas
GPBT	Greenhouse gas payback time
GWP	Global warming potential
FU	Functional Unit
HDPE	High density polyethylene
Imp	Optimum operating current
Isc	Short-circuit current
LCA	Life Cycle Analysis/Life Cycle Assessment
LCI	Life Cycle Inventory
M&O	Maintenance and operation
MG-Si	Metallurgical grade silicon
mono-Si	Monocrystalline silicon
multi-Si	Multicrystalline silicon
PCS	Power conditioning system
PV	Photovoltaic
PVC	Polyvinylchloride
PVT	Hybrid photovoltaic thermal system
SoG-Si	Solar grade silicon
STC	Standard test conditions
Vmp	Optimum operating voltage
Voc	Open circuit voltage
XLPE	Cross-linked Polyethylene
(GLO)	Global
{RER}	Europe
{RoW}	Rest of the world
{US}	United States

1. Introduction

Buildings consume more than 40% of the total energy consumption, as well as a significant fraction of non-renewable and non-recyclable building materials [1]. In order to make dramatic improvements in energy and natural resource conservation and improve the energy efficiency of buildings, new technologies are needed for the design and fabrication of the building envelope. As the photovoltaic (PV) technology has advanced in recent years, integrated technologies for harvesting solar energy, such as the Building-Integrated Photovoltaic (BIPV) system, have evolved as a promising solution for meeting energy and environmental challenges. The building integration schemes are gaining a worldwide recognition due to the considerable savings on building materials, construction, and operation. Although PV systems can convert to electricity the inexhaustible free solar energy, they can only transform part of the spectrum of solar irradiation into a manageable form for energy. Therefore, the next generation of solar energy panels needs to attain higher efficiencies of solar energy utilization, by harvesting two or three forms of solar energy, i.e., electricity, heat, and light.

This study examined a building-integrated system that simultaneously converts solar energy into electricity and heat, which is called a Building Integrated Photovoltaic Thermal (BIPVT) system. While the combination of two or three forms of energy capture is not a simple superposition of materials, it may provide a viable solution to significantly increase the overall energy efficiency by overcoming the limitations of each approach.

Hybrid photovoltaic thermal (PVT) collectors enable heat harvesting while improving the PV utilization efficiency by controlling the temperature of PV modules. Several research and development studies have been conducted over the last 25 years and have led to a number of innovative PVT systems and theoretical models with experimental validation [2]. There have been alternative approaches in PVT integration; among many others, there are air, water or evaporative collectors, monocrystalline/multicrystalline/amorphous silicon (mono-Si/multi-Si/a-Si), thin-film solar cells, flat-plate or concentrator types, glazed or unglazed panels, natural or forced fluid flow, stand alone or building-integrated features, etc. [2]. Because each approach or system has its own benefits and drawbacks, a holistic method is required to compare different systems. This study will subject a recently invented BIPVT system to a life cycle analysis (LCA). LCA is a recently developed scientific methodology for analyzing and quantifying the impact of a certain product or process on the environment, during its entire life time. As emphasized in the newly published LEED v4 green building rating standards of USGBC, the LCA of buildings and building products is becoming more and more important. Four major indicators will be used in the LCA conducted in this study, the global warming potential (GWP), fossil fuel consumption, greenhouse gas payback time (GPBT), and energy payback time (EPBT). It is hoped that the procedure and results of this analysis will provide future research and development direction for the examined BIPVT technology and, also, can be applied to other BIPVT systems for sustainability measurements, strategic planning and marketing.

2. System description

Although combined photovoltaic and thermal energy (PVT) systems have been developed for decades, very few systems are being used in the market due to the following potential problems [3]:

- Because most PVT panels bond multiple layers together, delamination between layers due to environmental temperature and moisture changes, severely reduce the life and efficiency of the panels[4], [5].
- For a PVT system with a heat collector, a temperature difference between warm indoor air and cold roof material may induce vapor condensation and degrade indoor thermal comfort [6].
- Exposure to weathering environments, may decrease solar material properties and structural strength with service time. Therefore, reliable and short-term test methods need to be developed to accurately evaluate the long-term performance of PVT.
- Conventional solar panels are configured as mounted equipment attached to the structural elements of the building skin, which is less than optimal due to material redundancy, potential leakage, extra installation and maintenance cost.
- Compared with PV panels, PVT systems are more complex and expensive, which imposes high risks for manufacturers to scale up the technologies for massive production and for customers to adopt the technology.
- In the absence of well recognized standards, although many PVT systems have been proposed in recent years, a majority of them were not deployed in the market due to some simple technical deficits and lack of rigorous test data; in the future, this can be avoided by standardization.

To address the above problems and develop a reliable method for the rapidly growing PVT technologies, a BIPVT system that can be used as multifunctional high-performance envelope, for next generation sustainable buildings has been recently developed. Figure 2.1 illustrates the design of the BIPVT panel. A solar cell layer below directly transform solar energy into electricity. They are bonded to a structural substrate by means of a functionally graded material (FGM) layer, in which water tubes are embedded to harvest heat energy, in the water flow through the tubes, and thus control the panel temperature. The substrate provides mechanical loading support and heat insulation of the building envelope. The multilayered solar panel is designed in such a way that layers of potentially shorter life-time expectancies can be easily replaced or be removed based on the sustainability measurement criteria, which can also be attained by alternative building materials and systems for building construction [7].

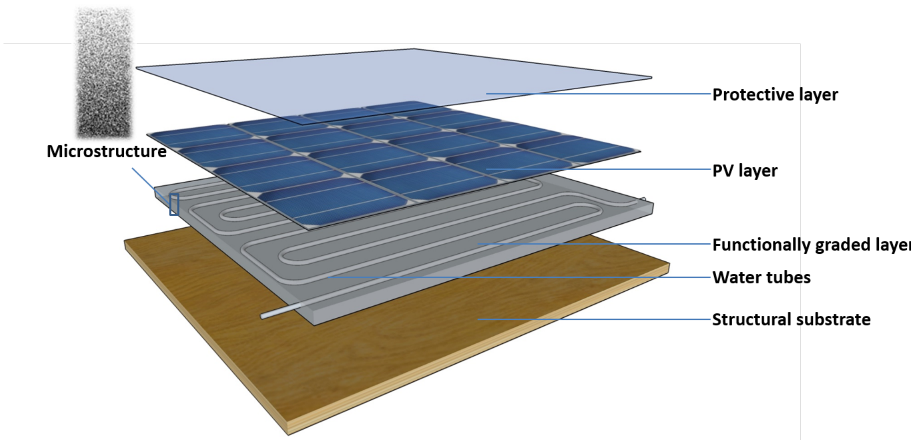

Figure 2.1: The hybrid solar roofing panel for PV and heat utilization[8]

The FGM layer gradually transits material phases from metal dominated to polymer materials. The water tubes are embedded in the top part of the FGM layer, where the high aluminum concentration creates high thermal conductivity so that heat can be immediately transferred to water tubes in all directions, except at the bottom part of FGM layer, which is made of pure high density polyethylene (HDPE) or polyvinylchloride (PVC) [9]. Due to the gradual change of the phase proportion of materials, only a small amount of aluminum powder is needed.

The proposed PVT panel can be integrated into building skin with water circulation, flow control, and heat storage and utilization systems. Solar irradiation is collected by BIPVT panels in forms of electricity and heat. Electricity is used locally or transmitted to the grid, while the heat can be stored or directly used as indoor or external heat supply such as floor heating, clean drying, and swimming pools. The innovations of the proposed PVT system are summarized as follows:

- Due to the temperature control by the water flow, the PV module can work at lower temperatures in the summer and thus stably obtain a higher efficiency for PV utilization.

- The hot water, whose temperature is partially controlled by the flow rate, can be directly utilized by water heating systems for indoor or external heat supply.
- Due to the temperature control on the roof, the room temperature can be significantly reduced and thermal comfort in the building can be much improved.
- In winter, a warm water flow can be used to remove ice and snow on the roof, clean solar panels, and thus restore and enhance solar energy utilization.
- A high percentage of Al powder allows heat to be rapidly transferred into water tubes, but below them the heat conduction is blocked by the HDPE and the lightweight concrete with recycled polymer.
- The thin film PV layer lowers the cost and improves the heat conduction and structural integrity within the panel, and protects the polymer materials underneath from UV radiation.

In addition, the performance of this system is significantly affected by the water flow. Using an accurate temperature sensing system and water flow rate control, the energy efficiency of the roofing system can be optimized. When days are warm and nights are cool, the heat captured by the water will be stored in a hot water tank. At night, this stored heat can be used in a radiant floor system or rejected to the cool night air by circulating the water through the panels. The substrate of the panel is designed as an integrated part of the building skin, allowing the panel to serve as both structural sheathing and waterproofing, eliminating material redundancies and the embodied carbon associated with those materials. The design of the substrate can be varied and optimized to suit the various wind and snow load conditions that occur throughout the United States and the world without adversely affecting the performance of the power generating elements[10].

3. Residential home integration

An example of the systems integration into a traditional residential architecture is illustrated in Figure 3.1. A simplified description of the construction is as follows: Connect the hybrid solar panels to the traditional roof framing. Seal the joints between the panels. Flash the roof edges and intersections, interconnecting the panels on the attic side to form fluid and electric circuits. Install the radiant heating systems. Install the hot water storage. Install the manifolds and connect the water circulation system. Install the system control unit. Once constructed and commissioned, the hybrid solar roofing system can run in an automatic mode.

The water circulation system in the attic space is connected as follows: Water is pumped into the roof through the major cold manifold just below the roof ridge. For the roof shown in Figure 3.1, 16 BIPVT 60cmX60cm (2'X2') panels are grouped together as one water circulation group. There are total four rows of such group. Water is pumped through four major cold water supply pipes place on the higher part of each group of panels. Flowing through each panel, the water is heated and then collected by hot water collection pipes on the opposite side of the row. This piping design and the double serpentine panel configuration will make the temperature distribution in each BIPVT panel and across the roof as uniform as possible.

For a typical house, only the south facing side would be used for this technology. For an average US home, with a south facing floor plan of about 125m^2 and a roof slope of 6/12, only 25% of the area will be installed BIPVT panels. With the current panel size of 60cmX60cm (2'X2'), 64 panels will be used to cover 25m^2 of the roof.

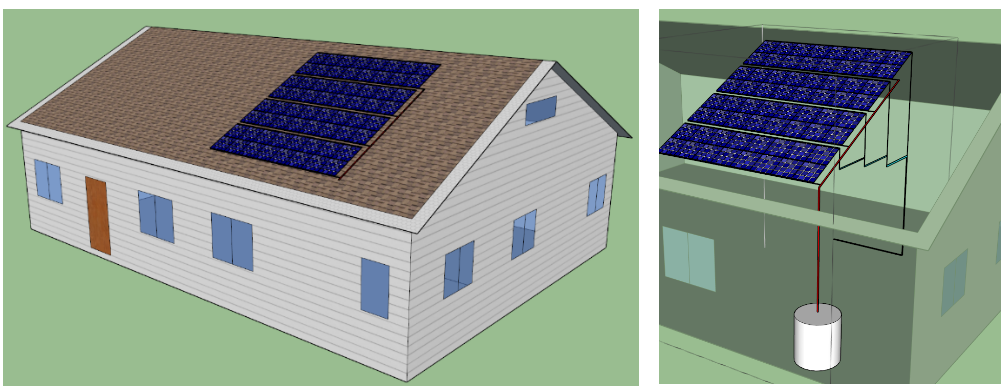

Figure 3.1: Plan of BIPVT panels on roof top, 25m^2 out of 125m^2

The 64 panels are divided into 16 groups of 4, connected in series to generate about 24V DC at their rated voltage (under STC). The groups of series, are connected in parallel to the charge controller and one inverter of 2.5 kVA capacity. The group detail is shown in Figure 3.2.

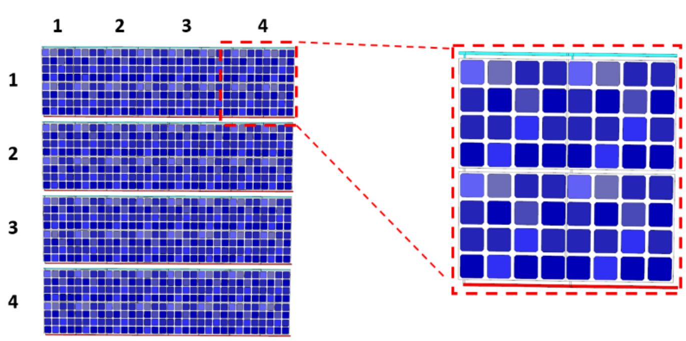

Figure 3.2: Method of BIPVT panels connection

4. Life cycle assessment

4.1. LCA methodology

Although the operation of PV systems consumes very little energy is consumed during PV manufacturing, balance of system (BOS) production, transport and installation, system disposal or recycling and other processes during its life cycle. LCA is very important to determine the overall energy efficiency and environmental impact of a system, and to compare different systems. LCA is defined as a technique for the compilation and evaluation of the inputs, outputs and the potential environmental impacts of a product system throughout its life cycle - from the extraction of resources, through the production of materials, parts and the product itself, the use of the product, and the management after it is discarded, either by reuse, recycling or final disposal and this methodology comprises four phases such as the goal and scope definition, inventory analysis, impact assessment and interpretation (ISO 14040, 2006) [11], [12]. LCA stages of PV system is shown in Figure 4.1. Specifically, the life cycle stages of PV systems mainly involve (1) the production of raw materials, (2) their processing and purification, (3) the manufacture of modules and balance of system (BOS) components, (4) the installation and use of the system, and (5) their decommissioning and disposal or recycling [13]. In this study, not all stages will be included as impacts of some stage are very small and data of some stages are either hard to find nor inexistent until now. The environmental impacts of the BIPVT system is assessed using the international standards for LCA, ISO 14040, 14044 and the methodology guidelines on LCA of PV issued by Task 12 of the International Energy Agency PVPS program [14], [15].

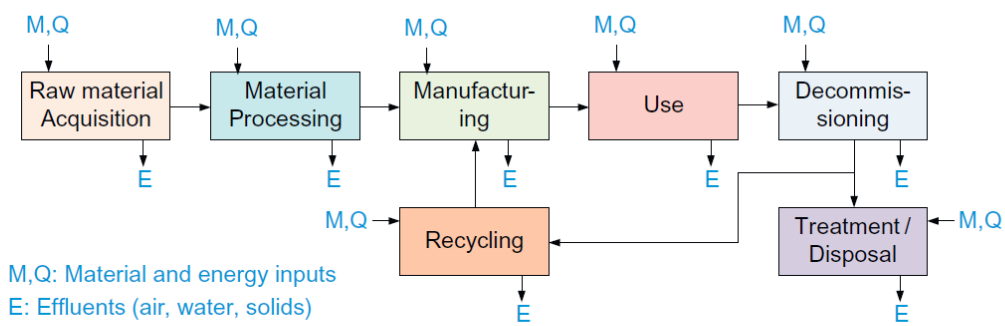

Figure 4.1: Flow of the life cycle stages, energy, materials and wastes for PV systems[16]

The analysis results include Global Warming Potential (GWP) and Cumulative Energy Demand (CED), which will be further interpreted as Greenhouse Gas Payback Time (GPBT), and Energy Payback Time (EPBT). The GHG emission is estimated through IPCC (Intergovernmental Panel on Climate Change) GWP 2013 100a method in the form of CO_2 equivalent within an integrated 100-year time horizon. The energy use calculation uses CED method which evaluates non-renewable energy inputs only. All energy type is interpreted to fossil fuel rather than renewable energy or nuclear energy. It is necessary to note that not only the used, or combusted energy, but also the embodied energy in the materials is included in the analysis. The concept of embodied energy is derived from the field of thermodynamics. For BIPVT systems, the embodied energy comprises indirect and direct energy. The direct energy may include that used on-site for the operation of power tools, while the indirect energy may include that used directly in the manufacture of PV modules or even the structural steel of the building [16, Ch. 7].

4.2. Data quality

According to ISO 14040, data quality requirements specify in general terms the characteristics of the data needed for the study. The data quality is important to the reliability of the study results and properly interpret the outcome of the study. A successful LCA is required to deal with a lot of real input and output data. However, it is difficult for the study to obtain all data in practice as the system is still not developed for commercial use. Until now, we have only a prototype system for laboratory test. Therefore, the BIPVT panel is modeled by laboratory data, which may be different from the industry data if it is massive manufactured. Like Kato et al. pointed out in a LCA study of PV modules, the energy consumption will decline as the scale of production rises [17]. Data qualities and sources used in this study are concluded in Table 4.1.

Table 4.1: Data qualities and sources of the study

Life cycle stages		Data quality	Data source
All stage	NY electricity mix	Secondary	US EIA
pre-manufacturing		Secondary	Ecoinvent etc.
Manufacturing	BIPVT panel	Primary	Carleton Laboratory
	PCS	Secondary	
	BOS	Primary + Secondary	Literature + Laboratory
Transportation		Primary + estimation	
Installation		Secondary+ estimation	Literature
Use		Primary + estimation	
Disposal		Not included in the study	

Environmental impact facts of most products or services were searched from SimaPro, a leading LCA software, which integrated a lot of Life cycle inventory (LCI) databases. The most useful database used in this study is called Ecoinvent, which is developed by the Swiss Centre for Life Cycle Inventories [18]. The Ecoinvent database is widely recognized as the largest and most consistent LCI database on the market. The Ecoinvent database is presented in a very transparent way and easy to use.

4.3. Process map & boundary

The system boundary in this study is defined as the pre-manufacturing, manufacturing, transportation and use stages. Installation, disposal, and recycling stages are excluded due to a lack of data. As shown in Figure 4.2, the system consists of three parts: BIPVT panel, PCS and BOS. Although transportation is only included in the last life cycle stage in the figure, it actually permeates throughout the whole life of the system. The environmental impacts of infrastructure for processing facilities and the processing facilities were not considered, which might lead to underestimation of the environmental impact caused by PV systems [12]. However, due to long-term use of them and large production capacity during their life cycle, there was little effect on the environmental impacts per unit of electricity [19].

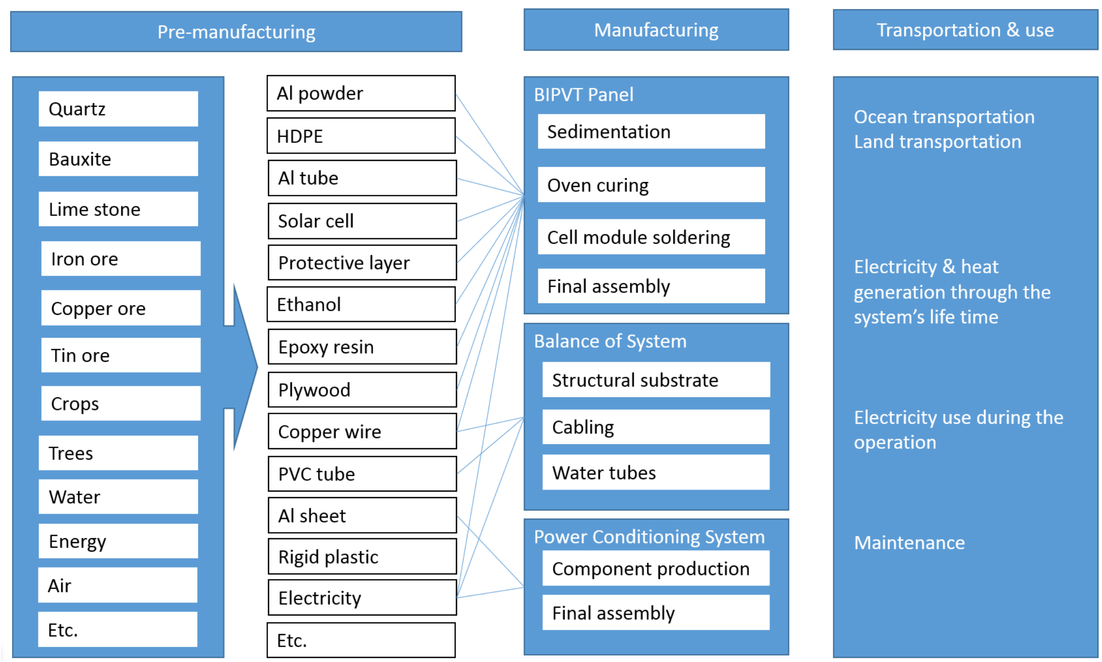

Figure 4.2: Life cycle stages of the study

The comparison between the BIPVT system and other PV systems will be done for a) the BIPVT panel, and b) for the entire BIPVT system. The BIPVT panel consists of protective layer, solar cell, Al bus bar, FGM panel with embedded water tubes, and adhesive (Figure 4.3). The BIPVT panel can be compared with framed PV module with the same surface area in terms of embodied energy and CO_2 equivalent during manufacture. The framed PV module is defined as the encapsulated and framed PV module or panel without any other mounting system, cabling, or power conditioning components. The BIPVT system consists of the BIPVT panel, structural substrate, and all other necessary BOS and PCS components. BIPVT system can be compared with similar scale PV systems with completed BOS and PCS components in terms of the conventional functional unit such as "kWh electricity produced" or "m^2 module" or “kWp rated power”.

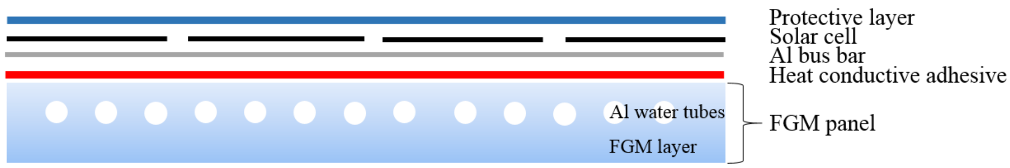

Figure 4.3: Schematic of the BIPVT panel structure

In addition, the transportation modes and distances between raw material provider, manufacturer, and end user are hard to evaluate. In our assumption, all the materials used are purchased within 100km from the manufacture factory except the solar cell, which were purchased from Guangdong, China. As a result, this study mainly considered the manufacturing stage of the BIPVT system, which is the most important and distinctive stage of the system’s life cycle. Packaging materials are also not given special attention, only packaging used for solar cell is included. No recycling material is considered in the study.

4.4. Functional unit & other assumption

In first step, the goal of the study and the main work hypotheses are defined. The key parameter to be fixed is the functional unit (FU), that is the quantified performance of a product system for use as a reference unit in LCA [20]. It is related to the service offered by the product. In the start sections, different functional unit may be used for different purpose, while the last conclusive functional unit is defined as 1 kWh of energy generated from a 2.5kWp electricity BIPVT system. Its operation lifetime expectancy and performance ratio is estimated as 25 years and 90% with degradation to 80%after 25 years according to the recommendation of the International Energy Agency (IEA) [15]. In fact, the lifespan of PV systems is usually due to the poor maintenance, which might lead to an underestimate of primary energy demand and environmental impacts per kWh generated by PV systems [15]. The energy content coefficients and service periods assigned for the BIPVT system, the installation, and M&O stages are assumed as shown in Table 4.2[16]. It is also worth to point out that conversion efficiency affected by temperature is rarely considered in the previous LCA studies, though it will be considered in detail in this study. However, the efficiency changes due to solar irradiation level is still not considered in this study.

Table 4.2: Energy content coefficients and service periods assigned for the BIPVT system

BIPVT system component	**Lifetime (years)**	**Assigned value for specific heat content**
BIPVT panel*	25	
Plywood substrate	30	
Foundation, array support, etc.	30	
Controller	10	
Inverter, safety factor 0.3	10	
PbA battery, depth of discharge 80%	5	
Installation	-	25 MJ/m^2
Hot water storage	25	
Pump	10	
Junction box, cabling, etc.	30	
M&O	-	5.4 MJ/m^2yr
* specific heat content of the components with asterisk will be interpreted in the following sections		

Some other assumptions are listed here: The lifetime of a group of components is the same. As soon as the lifetime of the group of components is over, they are replaced by a similar group of new components. The same technology is used to manufacture the items that are being replaced over the time period. So, the embodied energy does not change with the time period. The lifetime of all the other components of the BIPVT system is assumed to be the same as the BIPVT panel.

5. Life cycle inventory

The inventory of the BIPVT system will be analyzed step by step from the production of solar cells to power conditioning facilities. While only the facilities inside the red line was calculated in this LCA study. All the other facilities outside the box are either obligatory for a building (such as AC distribution center) or have very low impact to the final results. The definition of BOC and PCS should be clarify here because the unique function of the system (concluded in Figure 4.2). BOS, short for balance of systems, includes only substrate/foundation, cabling, and circulating water tubes. While PCS, short for power conditioning system, includes all the other electronic components such as inverter, controller, electricity/thermal storage, pump, and safety equipment, etc. Some studies don't consider either BOS or PCS due to their little influence on environmental impacts [21]. In addition, researchers usually separate the PV system into two parts as PV module and BOS, or three parts as PV module, frame, and BOS. Therefore, the BOS in some studies is basically the combination of BOS and PCS in my study. The reason I separate the system like it is because the BIPVT system has more power conditioning equipment than conventional PV systems. Previous studies show that, BOS accounted for additional ~0.2 years of EPBT of multi-Si PV system, ~5g CO_2-eq/kWh of GHG emissions, ~10mg/kWh of NOx emissions and ~18 mg/kWh of SOx emissions [22], [23]. Although the environmental effect of BOS is not significant, it is still calculated in the study. New York electricity mix and its carbon emission rate is obtained from US Energy Information Administration. The carbon emission rate is 1lb/MWh, which is about 0.4536g CO_2-e/kWh [24].

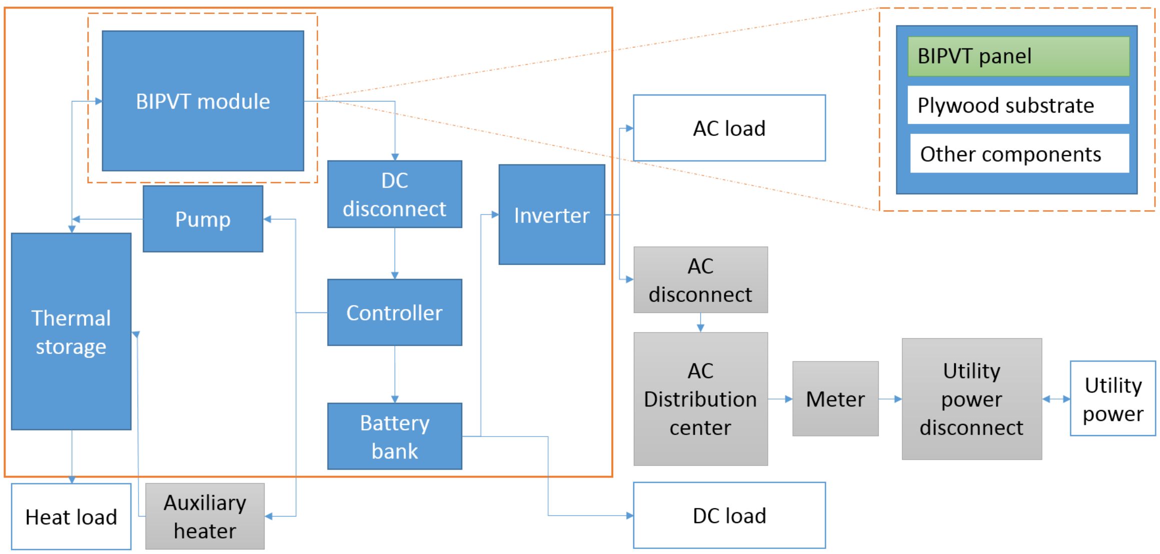

Figure 5.1: The schematic diagram of the BIPVT system and the boundary of this study

5.1. BIPVT panel

5.1.1. Solar cell

Solar cell is one of the most important components of the BIPVT panel. Although there are a lot of different types of solar cell now, monocrystalline silicon solar cell is used in the study. The solar cell for the lab testing was purchased from a Chinese company. The size of each cell is 125mm x 125mm, with a thickness of about 200µm. The efficiency of the solar cell is 16% to 18.6% under Standard Test Conditions (STC)[1]. The characteristics of one 125mm x 125mm solar cell provided by the manufacturer are shown in Table 5.1.

Table 5.1: Characteristics of one 125mm x 125mm solar cell in this study

General information			
Place of origin	Guangdong, China	Material	Monocrystalline silicon
Size	125mm x 125mm (5" x 5")	Efficiency	16%-18.6%
Thickness	200±20µm	Weight	6.7±0.5g
Optimum operating voltage (Vmp)	0.532V	Open circuit voltage (Voc)	0.634
Optimum operating	5.325A	Short-circuit current (Isc)	5.648A

[1] Standard Test Conditions (STC) : irradiance of 1000 W/m², spectrum AM 1,5 and cells temperature of 25°C

current (Imp)			
Max power (Pmax)	2.83W		
Temperature characteristics			
Operating temperature	-40°C to +85°C	α(Isc)	0.0461%/°C
γ(Pmax)	-0.3324%/°C	β(Voc)	-0.4384%/°C
Intensity dependence			
Irradiance[W/m²]	Open-circuit voltage[%]	Short-circuit current[%]	Maximum power[%]
1000	100.0	100.0	100.0
800	98.56	80.05	79.86
600	97.39	60.08	59.51
400	95.70	40.11	39.13
200	92.66	20.07	18.88

The life cycle stages of all commercial silicon-based PV modules (including mono-Si,multi-Si, a-Si, and ribbon techologies) are illustrated in the Figure 5.2. The processes being focused on in this section is the cell manufacturing processes as circled by the red line, which mainly include quartz reduction, metallurgical grade silicon (MG-Si) purification, solar grade silicon (SoG-Si) or electronic silicon (EG-Si) production, mono-Si or multi-Si crystallization, wafer sawing, and cell production. The transpotation, BOC, and all electronic components are not included in this section of study, but will be considered in tha later sections.

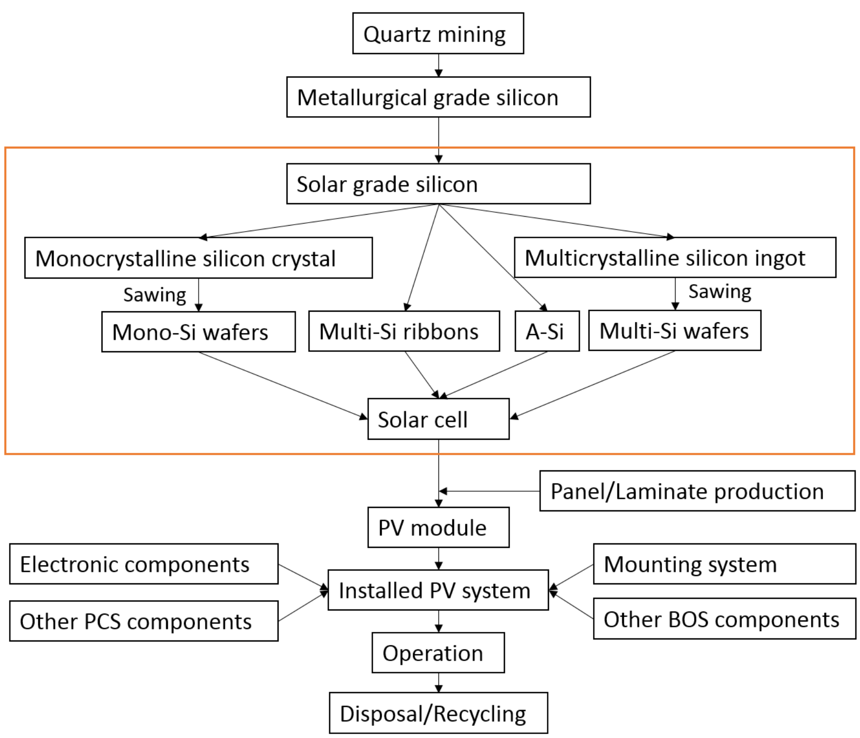

Figure 5.2: Life cycle stages of all silicon-based PV modules

The inventory data covers the material and energy consumptions involves all processes from silicon feedstock production via the production of solar grade silicon, wafers, ingots, and cells. All data were collected based on the up-to-date information, latest technology, and Chinese manufacturer. Most of the data were obtained from an article by Fu [21]. For the data cannot be found from the context of China, data from a report based on PV products in USA and Europe was used [22]. The energy consumption data referred to the report "Clean Production of Solar PV in China" published by Greenpeace[25]. The data of MG-Si production was from literature about MG-Si produced in China [26]. For the calculation, these data were implemented into the software Simapro, which was able to perform life cycle calculations and includes access to a rich database. Due to the lengthy of the inventory list, only the inventory data for the mono-Si solar cell production is listed in Appendix A. The FU in this section of calculation is 1m^2 of solar cell. The LCA results of the solar cells are interpreted as GWP and Cumulative Energy Demand (CED) as shown in Table 5.2. It illustrates that in the mono-Si technology has both the highest GWP and CED, while ribbon modules have the lowest ones during the cell production processes.

Table 5.2: GWP and CED results of 1m^2 silicon-based solar cell

	Mono-Si	**Multi-Si**	**Ribbon**
GWP (kgCO_2-e/m^2)	429.18	330.14	247.60
CED (MJ/m^2)	4595.7	3276.6	1957.4

5.1.2. FGM panel

The functionally graded material (FGM) panel as in our definition of scope is a solid FGM layer with thin wall aluminum tubes casted within. The functionally graded material (FGM) layer is manufactured with the vibration method in the laboratory by mixing aluminum powder, high density polyethylene (HDPE) power, and ethanol. Because Al and HDPE have significantly different specific gravities (2.7 and 0.95, respectively) over a range of size distribution (100-600μm and 3-100μm, respectively), the two types of powders will fall down at different velocities and thus create a graded microstructure. When a desired graded microstructure forms with thin wall Al tubes inside, the fluid is filtered. Heat up the graded powder mix in a vacuum oven, melt the HDPE powder, apply a pressure for mold casting, and cure it to the ambient temperature, in which procedure, a solid FGM panel with Al tubes inside can be obtained. The FGM panel manufacture comprises the following elements and processes, which are clarified in the flow chart below. The in-depth inventory and process analysis of the manufacture of one 60cm x 60cm (2' x 2') panel listed in Table 5.3. Since Al casting or processing cannot be found in the database, brass casting data is used in the study. It is essential to point out that the manufacture method used here is a relatively small scale method in laboratory. For a more industrial-like estimation, all equipment and facilities for manufacture will be assumed to be in full loaded usage. The results of the GWP and CED to manufacture one 60cm x 60cm (2' x 2') FGM panel is listed in Table 5.4, which clearly tells that the material contributes the most energy consumption and environmental impact in the overall inventory.

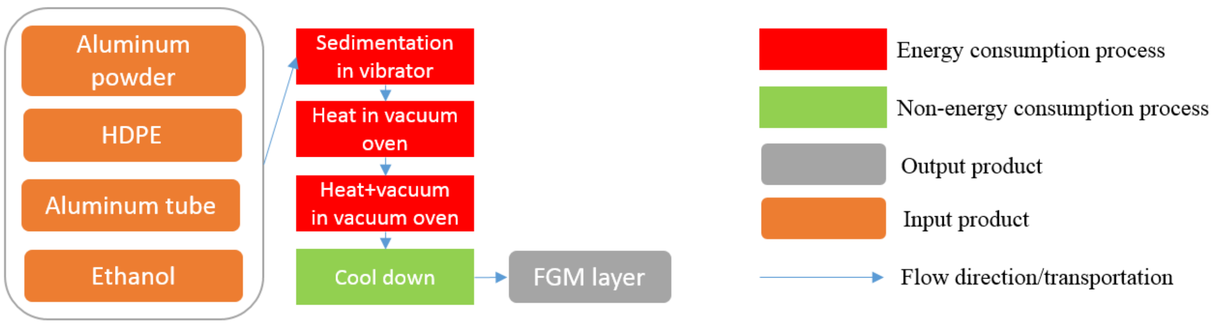

Figure 5.3: FGM panel lab manufacture flow chart

Table 5.3: Inventory of materials and processes to manufacture one 60cm x 60cm (2' x 2') FGM panel

Component	**SimaPro process**	**Database**	**Mass (g/panel)**	**Energy (Wh/panel)**
Material				
Al powder	Aluminum, primary, ingot, at plant	USLCI	2786	
Al powder manufacture	Casting, brass {GLO}	Ecoinvent		498.61
HDPE	High density polyethylene resin, at plant	USLCI	2849	
Al tube	Aluminum, primary, ingot, at plant	USLCI	144.07	
Al tube manufacture	Casting, brass {GLO}	Ecoinvent		28.73
Ethanol	Ethanol, without water {US}	Ecoinvent	2987	
Transportation				
Land transportation	Transport, truck 10-20t, EURO5, 80%LF, empty return/GLO Energy	Ecoinvent	6000	
Process				
Sedimentation	Electricity mix, US			6.71
Heat	Electricity mix, US			600
Vacuum	Electricity mix, US			480

Table 5.4: GWP and CED to manufacture one 60cm x 60cm (2' x 2') FGM panel

	Material	**Process**	**Transportation**	**Overall**
GWP (kgCO_2-e/panel)	40.45	0.66	0.15	41.27
CED (MJ/panel)	566.79	15.26	2.184	584.24

5.1.3. Final assembly

In the final assembly, solar cells are first solder together to be a 4 x 4 module. Then, the module is covered by a protective glazing layer and adhered on to the FGM panel. All the inventories of this step are listed in Table 5.5. Combining with the previous calculation, GWP and CED of one studied BIPVT panel using different solar cells are shown in Table 5.6. It is clear that during the manufacture stage of the whole life cycle, mono-Si based BIPVT panel consumes the most energy and the ribbon based consumes the least. As shown in Figure 5.4, CED of ribbon BIPVT in the manufacture stage is only 62% of that of mono-Si BIPVT. The reason is simply because all the other components used for the systems are almost the same apart from the solar cell. Additionally, solar cell contributes the most GHG emission and energy use during manufacture (60%-70%).

Table 5.5: Inventory of materials and processes to assemble one 60cm x 60cm (2' x 2') BIPVT panel

Component	**SimaPro process**	**Database**	**Mass (g/panel)**	**Energy (Wh/panel)**
Material				
FGM panel			5000	
Solar cell			116.67	
Protective layer	Flat glass, uncoated {GLO}	Ecoinvent	0.202	
Ethyl Vinyl Acetate	Ethyl acetate {GLO}	Ecoinvent	0.36	
Galvanized cooper strips	Aluminum, primary, ingot, at plant	USLCI	30.29	
Stripe manufacture	Casting, brass {GLO}	Ecoinvent		6.04
Thermal conductive adhesive	Flame retardant epoxy resin	Ecoinvent	78.46	
	catalyst 150 (polyoxypropylenediamine)	Ecoinvent	13.34	
Solder core	Solder, bar, Sn63Pb37, for electronics industry	Ecoinvent	4.72	
Transportation				
Ocean transportation	Transport, freight, sea, transoceanic tanker {GLO}	Ecoinvent	0.117	
Land transportaiton	Transport, truck 10-20t, EURO5, 80%LF, empty return/GLO Energy	Ecoinvent	0.328	
Process				
soldering	Electricity mix, US			10

Table 5.6: GWP and CED of one 60cm x 60cm (2' x 2') BIPVT panel by using different solar cells

	Mono-Si BIPVT	**Multi-Si BIPVT**	**Ribbon BIPVT**
GWP (kgCO_2-e/panel)	153.84	129.08	108.45
CED (MJ/panel)	1812.74	1482.96	1053.16

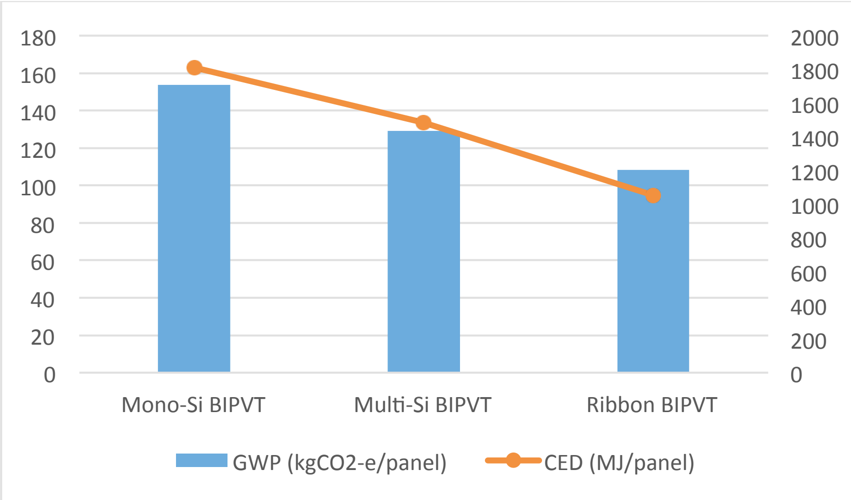

Figure 5.4: Comparison of GWP and CED of one 60cm x 60cm (2' x 2') BIPVT panel by using different solar cells

5.2. Balance of system

As it is described in the previous section, in this study, BOS contains water pipe outside the BIPVT panel, cabling, and other components such as structural support substrate, valve and screw, etc. The data for BOS was estimated according to the laboratory model and the residential building integrated system drawing. The material quantity and process energy listed below are both based on the amount of one unit of 2.5kWp BIPVT system.

5.2.1. Water pipe

According to the system drawing, about 170m flexible PE pipe is used for cold water supply, and 30m EPED insulated flexible hot water pipe is used for water return. The outer diameter of the water supply pipe is 8mm, and the thickness is 1.5mm. The outer diameter water the water return pipe is 32mm with a 5mm thick insulation layer and steal pipe inside.

Table 5.7: Water pipe inventory of the BIPVT system

Component	**SimaPro process**	**Database**	**Mass (kg/system)**	**Energy (WJ/system)**
PE water supply pipe[2]				
PE pipe	High density polyethylene resin, at plant	USLCI	3	
PE pipe extrusion	Extrusion, plastic pipes {GLO}	Ecoinvent		16.4
EPDM pre insulated hot water pipe[3]				
Steel	Steel, low-alloyer {GLO}	Ecoinvent	25	
Pipe drawing	Drawing of pipe, steel {GLO}	Ecoinvent		88.25
EPED	High density polyethylene resin, at plant	USLCI	5	

[2] http://www.alibaba.com/product-detail/special-PERT-PEX-thin-wall-pipe_1258415800.html?s=p
[3] http://www.alibaba.com/product-detail/dn16-epdm-pre-insulated-solar-flexible_1320265798.html?s=p

EPED extrusion	Extrusion, plastic pipes {GLO}	Ecoinvent		27.4
Transportation				
Land transportation	Transport, truck 10-20t, EURO5, 80%LF, empty return/GLO Energy	Ecoinvent	34	

5.2.2. Cabling

It is estimated a total of 60m cable is used in the system, including 55m DC and 5m AC cable. The cable is made from copper with outer diameter of 6.4mm and conductor diameter of 2.6mm. Both cables are jacketed with Cross-linked Polyethylene (XLPE), and the inner conductor is copper. Half length of the cable is enclosed inside electrical conduit. Two types of electrical conduit are employed in the BIPVT system: Rigid Metal Conduit (RMC) and Flexible Metal Conduit (FMC), both of which are composed of steel with outer diameter of 2.5cm.

Table 5.8: Cabling inventory of the BIPVT system

Component	SimaPro process	Database	Mass (kg/system)	Energy (WJ/system)
RMC and FMC				
Steel	Steel, low-alloyer {GLO}	Ecoinvent	30	
Pipe drawing	Drawing of pipe, steel {GLO}	Ecoinvent		105.9
DC and AC cable[4]				
Copper	Copper {GLO}	Ecoinvent	2.7	
Wire drawing	Wire drawing, copper {GLO}	Ecoinvent		22.46
XLPE	High density polyethylene resin, at plant	USLCI	0.3	
Jacket extrusion	Extrusion, plastic pipes {GLO}	Ecoinvent		1.64
Transportation				
Land transportation	Transport, truck 10-20t, EURO5, 80%LF, empty return/GLO Energy	Ecoinvent	34	

5.2.3. Other components

It is assumed that 10kg steal components are used based on the estimation of 256 screws, each screw weights 40g in the system. Another 10kg aluminum components and 5kg copper components are estimated to be used in the system. The Table 5.10 shows the overall GWP and CED of the system's BOS, among which plywood accounts the most (56% GWP and 43% CED, shown in Figure 5.5).

Table 5.9: Other components inventory of the BIPVT system

Component	SimaPro process	Database	Mass (kg/system)	Energy (WJ/system)
Support substrate				
Plywood	Plywood, for outdoor use {RER}	Ecoinvent	326.1	
Valves and screws				

[4] http://www.alibaba.com/product-detail/TUV-PV-DC-Single-Core-Twin_1843557861.html?s=p

Copper	Copper {GLO}	Ecoinvent	5	
Copper working	Metal working, average for copper product manufacturing {GLO}	Ecoinvent		186.5
Steel	Steel, low-alloyer {GLO}	Ecoinvent	10	
Steal working	Metal working, average for steal product manufacturing {GLO}	Ecoinvent		260
Aluminum	Aluminum, primary, ingot, at plant	USLCI	10	
Aluminum working	Metal working, average for aluminum product manufacturing {GLO}	Ecoinvent		462
Transportation				
Land transportation	Transport, truck 10-20t, EURO5, 80%LF, empty return/GLO Energy	Ecoinvent	352	

Table 5.10: Inventory table of the system's BOS

	Water pipe	**Cabling**	**Others**	**Overall**
GWP ($kgCO_2$-e/system)	97.37	92.10	747.46	936.93
CED (MJ/system)	1338.00	922.86	6466.62	8727.48

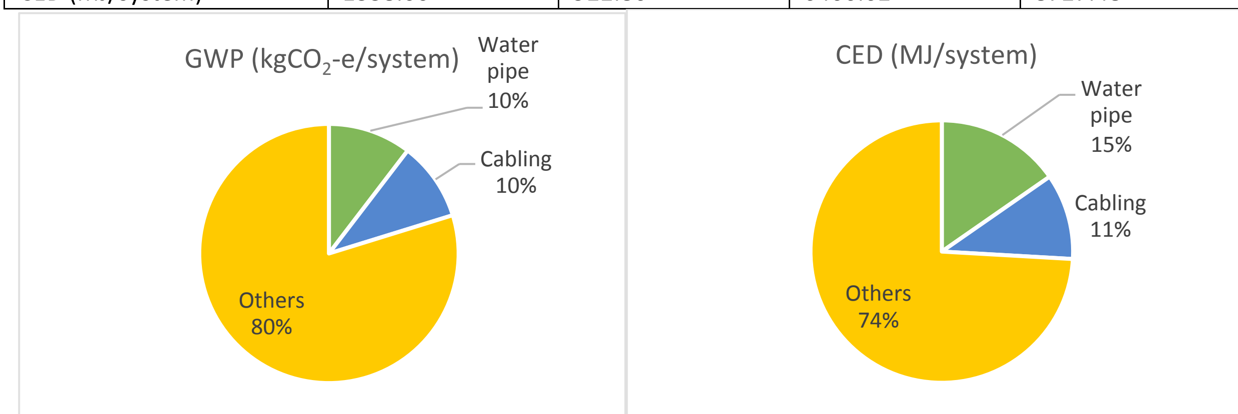

Figure 5.5: Contribution of GWP and CED of each parts of the BIPVT system's BOS

5.3. Power conditioning system

The power conditioning system here is defined as the equipment used in the system to ensure it works properly. The main PCS components in this study are inverter, controller, water circulation pump, and safety equipment. The most important equipment are inverter and controller. Obtaining data on the PCS production is challenging due to the large number of components. In this study, assumptions were made based on some previous studies and guideline [16], [27], [28]. The target product was a 2.5kW PCS and the time-related boundary for data collection was 2010. The material quantity and process energy listed below are also based one unit of 2.5kW BIPVT system.

5.3.1. Inverter & controller

Inverter is used to convert power from direct current (DC) to alternating current (AC), and the inverter used in the project is a 2.5kVA residential inverter with the input DC source of 24V to 48V and AC output of 110V. As the rated capacity of the inverter (P_{inv}) is given by:

$$P_{inv} = P_{LD}(1 + SF)$$

Where SF is the safety factor, which is usually considered as 0.3, the peak electricity load demand (P_{LD}) of the consumer depends on the BIPVT system should be less than 1.9kW. The inventory table of the 2.5kVA inverter is listed below. The controller firstly is used to regulate the rate of flow of electricity from the PV array to the battery and the load. Second, it is used to control water flow by adjusting the pumps. The GWP and CDE and the controller is assumed to be the same as the inverter.

Table 5.11: 2.5kVA inverter inventory of the BIPVT system

Component	SimaPro process	Database	Mass (kg/system)	Energy (WJ/system)
Metal components mass fraction				
Copper	Copper {GLO}	Ecoinvent	3	
Aluminum	Aluminum, primary, ingot, at plant		4.21	
Plastic components				
HDPE	High density polyethylene resin, at plant	USLCI	0.951	
Printed circuit boards				
Integrated circuit-logic	Integrated Circuit, logic type {GLO}	Ecoinvent	0.079	
Integrated circuit-memory	Integrated Circuit, memory type {GLO}	Ecoinvent	0.079	
Casting compound				
Silicone	Silicone product {GLO}	Ecoinvent	0.0793	
Rubber components				
Synthetic rubber	Synthetic rubber {GLO}	Ecoinvent	0.634	
LCD-display				
HDPE	High density polyethylene resin, at plant	USLCI	0.634	
Process				
Manufacturing energy	Electricity mix, US	Ecoinvent		33.84
Transportation				
Land transportation	Transport, truck 10-20t, EURO5, 80%LF, empty return/GLO Energy	Ecoinvent	9.7	

5.3.2. Pump & storage

It is assumed two circulating pumps are used in the system, which should overcome the head pressures every time it turns on. Moreover, the pump must be compatible with the BIPVT system in terms of its size, hydraulics, speed storage, maintenance free, high efficiency and low power consumption [29]. The hot water storage is used to store excessive hot water generated by the system. The technical details of the circulating pump and hot water storage is listed in Table 5.12. The GWP and CED are also listed in the table, which are directly found from the Ecoinvent database.

Table 5.12: Specifics of circulating pump and hot water storage

			GWP ($kgCO_2$-e/p)	CED (MJ/p)
Circulating pump	Max. delivery	6m	5.74	69.3
	Max. operating pressure	10bar		
	Permissible temperature range	-10 to 110 ^oC		
Hot water storage	Capacity	600l	748	8630

5.3.3. DC disconnect

Automatic and manual safety disconnects protect the wiring and components. In the case of grid-connected systems, safety disconnects ensure that the generating equipment is isolated from the grid, which is important for the safety of people. The DC disconnect used in the system is steel-enclosed, with three pole, fused safety switches.

Table 5.13: DC disconnect inventory of the BIPVT system

Component	SimaPro process	Database	Mass (kg/system)	Energy (WJ/system)
Copper terminal blocks				
Copper	Copper {GLO}	Ecoinvent	0.013	
Steel superstructure				
Steel	Steel, low-alloyer {GLO}	Ecoinvent	3.5	
Steal extrusion	Impact extrusion of steel, warm, initial warming {GLO}	Ecoinvent		26.8
Plastic fuse holder/handle				
HDPE	High density polyethylene resin, at plant	USLCI	0.5	
Injection molding process	Injection moulding {GLO}	Ecoinvent		302.9
Process				
Enamelling	Enamelling {GLO}	Ecoinvent	0.245m^2	41.16
Transportation				
Land transportation	Transport, truck 10-20t, EURO5, 80%LF, empty return/GLO Energy	Ecoinvent	17	

5.3.4. Battery bank

Batteries are the energy storing devices generally employed for solar applications. They store the electricity to meet load demand during off-sunshine hours when the modules are generating insufficient or no power. To provide electricity over longer periods, PV systems require deep-cycle batteries. Lead-acid batteries are usually designed to gradually discharge and recharge 80% of their capacity hundreds of times. In the BIPVT system, a 24V, 1000Ah battery is used, whose GWP and CED are estimated through battery category data in Ecoinvent database. As shown in Figure 5.6, the hot water storage has the most environmental effect among all of the PCS components.

Table 5.14: Inventory table of the system's PCS

	Inverter	Controller	Pump	Water strorage	DC disconnect	Battery[5]	Overall
GWP ($kgCO_2$-e/system)	183.40	183.40	11.48	748	12.38	401.94	1540.6
CED (MJ/system)	2501.89	2501.89	138.6	8630	175.89	5273.1	19221.37

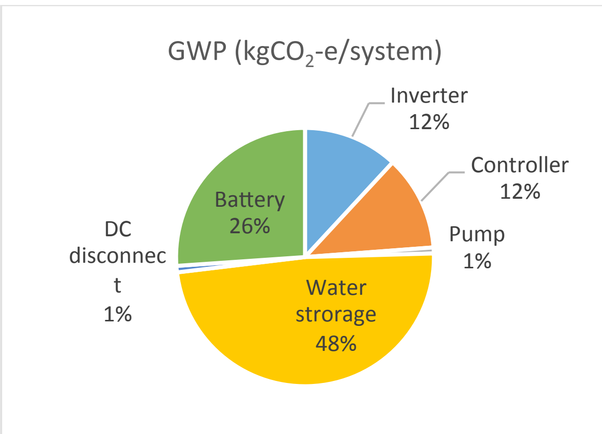

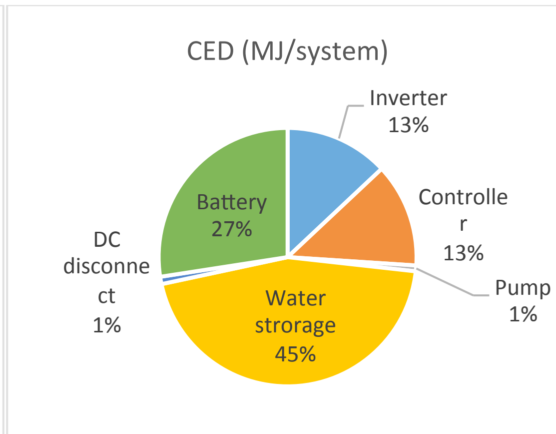

Figure 5.6: Contribution of GWP and CED of each parts of the BIPVT system's PCS

5.4. Alternative roof structure

The alternative roof structure, which the 2.5kWp electricity power BIPVT system entirely replaces at the rooftop, blankets about 30m^2 of the overall roof area. When examining the impact of the BIPVT system, we credit the impact of the alternative system as an "avoided product" because in effect, the rooftop BIPVT module fully replaces the covering part of the alternative roof structure. The embodied energy of roof structure varies of alternatives are available in the market. The specific energy contents of the eight roof structures suggested by Agrawal and Tiwari are similar with an average of 461.1MJ/m^2 (listed in Table 5.15) [16]. However, the structures of the listed roof types are slightly different from those are used in traditional US residential houses. Additionally, only part of the roof structure can be replaced by the BIPVT system. The inventory table (Table 5.16) is built according to the section drawing of a typical

[5] http://www.alibaba.com/product-detail/24v-1000ah-battery-for-telecom-and_1856220817.html

US residential house roof structure as shown in Appendix B. The BIPVT panel can replace the components of the roof structure above insulation as illustrated on the right hand side of the table.

Table 5.15: Specific energy content of different roof systems

Type of roof	MJ/m^2	Type of roof	MJ/m^2
RC slab	730	Burnt clay brick masonry vault roof	575
SMB filler slab roof	590	SMB masonry vault roof	418
RC ribbed slab roof	491	Mangalore tile roof	227
Composite brick panel roof	500	Ferroconcrete roof	158
Average	461.1		

Table 5.16: Inventory of replaced part of the alternative wood shake and clay tile roof structure

Material	Amount	GWP (kgCO_2-e)	CED (MJ)
Clay tile	60kg	27.06	298.2
Tile batten	0.34m^3	350.2	2550
InSkew fixing	5kg	10.05	98
Breathable membrane	30m^2	27	435
Overall		414.31	3381.2

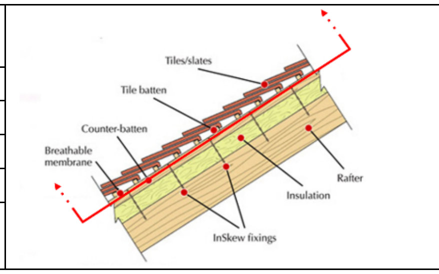

6. Lab testing

6.1. Experiment description

11 thermal couples are attached on the surface of the solar panel to evaluate the temperature distribution, as shown in Figure 6.1. For the data analysis conveniences, the sensor point number sequence follows the water flow direction. Number 1 and 11 thermal couples are attached in the inlet and outlet water tube to test the water temperature difference. The solar panels were tested in a solar room equipped with a metal halide lamp, which can provide irradiation up to 4KW/m^2. The panel was fixed on a wood frame so that the panel surface was normal to the irradiation. A pyranometer was used to measure and calibrate the solar irradiation. A mass flow meter was used to control the cooling water flow rate. The experimental data was collected with the data acquisition system.

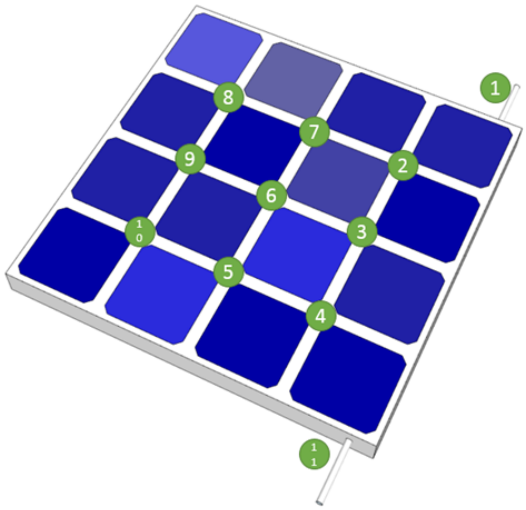

Figure 6.1: Position of thermal couples

The performance of the solar panels was characterized in the following way: The solar panels were put in the solar room under irradiations of 620W/m^2, 800W/m^2 and 1000W/m^2. Before the water flow was started, the solar panel surface temperature was automatically measured with an interval of 2s until the panel reached it is maximum temperature and stabilized. Then the water flow was introduced with the inlet water temperature of about 20^{o}C. The flow rate was controlled by the mass flow meter from 30ml/min to 150ml/min. The testing room temperature is measured simultaneously. The PV cell and water temperatures were recorded continuously until the panel temperature stabilized again.

6.2. Experiment results

Table 6.1 shows the conclusion of water temperature increase and panel surface temperature decrease under different solar irradiation and water flow rate. It is observed that in different irradiation, the testing room air temperature also changes. In order to make a more accurate assumption for the following system performance research, I concluded these changes in Table 6.2. The solar cell efficiency includes in the table only takes its surface temperature as a consideration.

Table 6.1: Water temperature increase and panel surface temperature decrease in different testing conditions

Solar irradiation (w/m^2)	**Water flow rate (ml/min)**	**Water temp. increase ΔT (^{0}C)**	**Panel surface temp. decrease ΔT (^{0}C)**
620	30.5	26.5	12.7
	59.2	22.9	19.6
	92.5	17.7	22.2
	117.3	14.9	23.9
800	31.2	32.2	15.7
	53.6	27.5	22.6
	93.2	21.3	26.9

	122.4	19.1	28.9
	150.2	14.5	30.6
1000	29.6	38.3	14.3
	61.6	28.7	24.6
	92.8	23.8	29.7
	123.5	22.0	32.6
	147.4	16.7	33.9

Table 6.2: Relationship of solar irradiation, testing room temperature, and cell efficiency

Solar irradiation (w/m^2)	**Testing room temp. (^0C)**	**Max. panel surface temp. w/o water flow T_c (^0C) & η_c**	**Water flow rate (ml/min)**	**Panel surface temp. after water flow T_c' (^0C) & η_c'**
620	26	52 (16.5%)	30.5	39.3 (17.2%)
			59.2	32.4 (17.7%)
			92.5	29.8 (17.8%)
			117.3	28.1 (17.9%)
800	30	62 (15.9%)	31.2	46.3 (16.8%)
			53.6	39.4 (17.2%)
			93.2	35.1 (17.5%)
			122.4	33.1 (17.6%)
			150.2	31.4 (17.7%)
1000	34	70 (15.4%)	29.6	55.7 (16.3%)
			61.6	45.4 (16.9%)
			92.8	40.3 (17.2%)
			123.5	37.4 (17.4%)
			147.4	36.1 (17.4%)

In the table above, it is clear that the maximum panel surface temperatures with and without water flow are related with the room temperature and solar radiation. In order to predict the panel surface temperature under different weather conditions, an energy balance model is assumed to be the following equation, where the interfacial loss between the solar cell and FGM panel is neglected:

$$[solar\ energy\ exposed\ on\ the\ panel\ surface] = [reflection\ energy\ loss] + [radiation\ energy\ loss] + [convection\ heat\ loss] + [solar\ cell\ electricity\ production] + [energy\ transferred\ to\ FGM\ panel]$$

The reflection, radiation, and convection energy loss can be calculated as:

$$\mathrm{E}_{ref} = R \cdot E_{in}$$

$$\mathrm{E}_{rad} = \varepsilon s\left({T_c}^4 - {T_a}^4\right)$$

$$\mathrm{E}_{con} = h_o(T_c - T_a)$$

by using the reference value of R=0.12, ε = 0.6, s = 5.67 ×10^{-8} W/m^2K^4 , and h_o =5W/m^2K, where R, ε, s, and h_o are the average surface reflective coefficient, emissivity of silicon, Stefan–Boltzmann constant, and convection coefficient of air, respectively [30], [31]. T_c is the panel surface temperature, T_a is the ambient temperature, E_{in} is the solar energy exposed on the panel surface. It is assumed that the actual energy conversion efficiency used for calculation here is only related with solar cell temperature. The solar cell efficiency and solar energy generation could be calculated as:

$$\eta = \eta_{STC}\left(1 - \phi_t(T_c - T_{STC})\right)$$

$$E_{PV} = \eta E_{in}$$

by using the manufacturer's value of η_{STC}=18.1%, $\phi_t = 0.3324\%/°C$, $T_{STC} = 25°C$, where η_{STC}, ϕ_t, and T_{STC} are solar efficiency, temperature coefficient, and ambient temperature of standard test conditions. Therefore, the energy transferred to FGM panel with or without water flow, which is defined as leftover energy:

$$E_{leftover} = E_{in} - E_{ref} - E_{rad} - E_{con} - E_{PV}$$

According to the experiment data, the results are listed in the table below. The leftover energy ($E_{leftover}$) generally includes two parts: energy transferred to water flow (E_{water}) and energy loss in various ways (E_{loss}). Table 5.3 lists the results of energy balance without water flow from 600W/m^2 to 1000W/m^2 of solar radiation. The percentage of leftover energy to the incoming energy is about 34% based on the calculation, which is taken as an constant in the future panel surface temperature prediction under different weather conditions.

Table 6.3: Energy balance and surface temperature in different experiment conditions

E_{in} (w/m^2)	T_a (^{0}C)	T_c (^{0}C)	η	E_{ref} (w/m^2)	E_{rad} (w/m^2)	E_{con} (w/m^2)	E_{PV} (w/m^2)	$E_{leftover}$ (w/m^2)	$E_{leftover}$/ E_{in}
600	26	52.0	16.5%	72	107.6	130.0	98.9	191.5	31.9%
650	27	54.6	16.3%	78	116.2	137.9	106.1	211.8	32.6%
700	28	56.8	16.2%	84	123.4	144.2	113.3	235.2	33.6%
800	30	62.0	15.9%	96	141.7	160.0	127.0	275.3	34.4%
900	32	65.8	15.6%	108	154.0	169.2	140.8	328.0	36.4%
1000	34	70.0	15.4%	120	168.7	180.0	153.9	377.4	37.7%

Based on the energy balance model and the leftover energy constant, panel surface temperatures in different ambient temperatures and radiation levels are predicted and listed as follows. This table will be used for annual energy generation estimation when deciding start time and rate of water flow.

Table 6.4: Predicted panel surface temperature without water flow in different weather conditions

	E_{in} (w/m^2)													
T_a	200	250	300	350	400	450	500	550	600	650	700	800	900	1000
(^{0}C)	T_c (^{0}C)													
-10	4	7.4	10.8	14.1	17.4	20.6	23.8	26.9	30	33	36.1	42	47.7	53.4
0	13.5	16.8	20	23.2	26.3	29.4	32.5	35.5	38.5	41.5	44.4	50.1	55.6	61.1
10	23	26.1	29.2	32.3	35.3	38.3	41.3	44.2	47	49.9	52.7	58.2	63.5	68.8
20	32.5	35.5	38.5	41.4	44.3	47.2	50	52.8	55.6	58.3	61	66.3	71.5	76.6
30	42	44.9	47.7	50.6	53.4	56.1	58.8	61.5	64.2	66.8	69.4	74.5	79.5	84.4

7. Performance assessment

7.1. Energy generation

Energy generation was estimated in three locations in the USA according to the 2010's solar radiation and weather data obtained from National Renewable Energy Laboratory and National Climatic Data Center. The three locations are Phoenix, Albany, and Duluth. The reason of choosing these three locations because they represent three climate types based on ASHRAE Climate Zones Map as shown in Figure 7.1. Phoenix represents zone 1, 2, and 3, Albany represents 4, 5, and Duluth represents 6, 7.

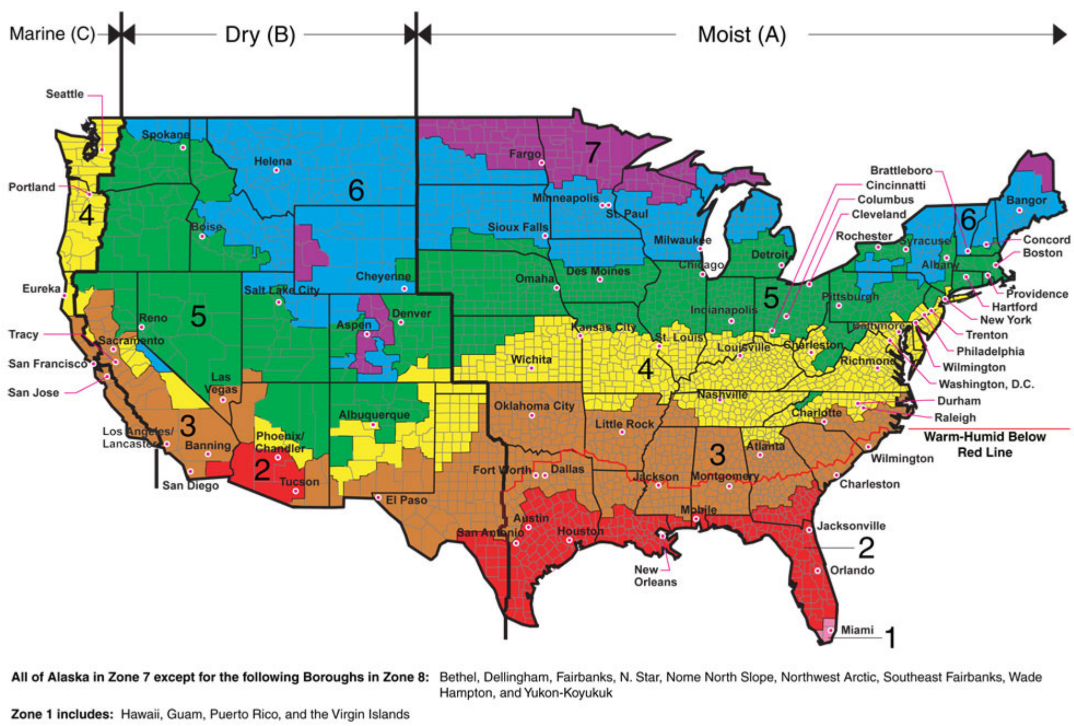

Figure 7.1: ASHRAE Climate Zones Map

Based on Table 6.4 (the predicted panel surface temperature without water flow in different weather conditions), and the experiment results, a table is constructed to determine the amount of water flow and water temperature increase in different weather conditions. It is assumed that by implementing such water flow strategy, the solar cell efficiency can be always maintained at 17.1%.

Table 7.1: Recommended water flow rate in different weather conditions

	E_{in} (w/m^2)										
	<200	200-300	300-400	400-500	500-600	600-700	700-800	800-900	900-1000	>1000	
T_a (^{0}C)	**Water flow rate (ml/min)**										**Water temp. increase ΔT (^{0}C)**
<-10	0	0	0	0	8	12	15	25	36	53	10
(-10~0]	0	0	0	0	10	15	18	30	53	72	13
(0~10]	0	0	8	12	15	25	40	62.5	82	100	18
(10~20]	0	10	13	21	32	48	67	86	106	134	18
>20	0	12	15	25	36	53	72	91	112	140	18

The power incident on the BIPVT panel depends not only on the power contained in the sunlight, but also on the angle between the panel and the sun. When the absorbing surface and the sunlight are perpendicular to each other, the power density on the surface is equal to that of the sunlight. However, as the angle between the sun and the fixed roof surface or BIPVT panel is continually changing, the power density on the fixed BIPVT panel is less than that of the incident sunlight. The amount of solar radiation incident on the BIPVT panel surface is the combination of the direct solar radiation which is perpendicular to the module surface and diffuse solar radiation, regardless of reflection or other radiation. The following figure (Figure 7.2) shows how to calculate the direct radiation incident on a tilt surface ($S_{surface}$) given either the radiation measured on horizontal surface ($S_{horizontal}$) or the radiation measured perpendicular to the sun ($S_{incident}$).

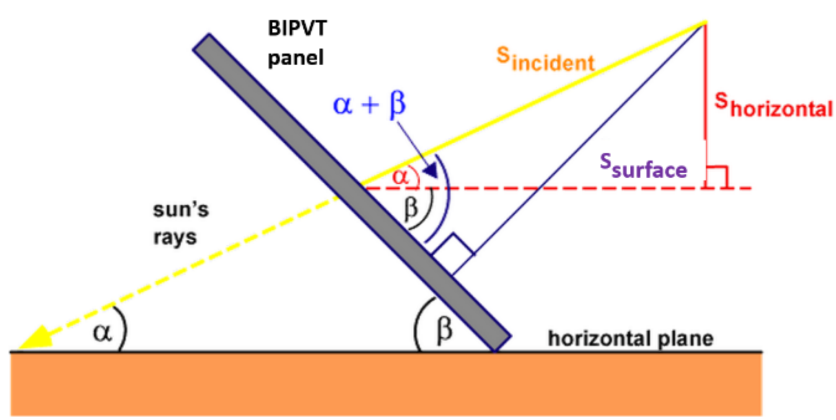

Figure 7.2: Relationship between incident solar radiation, radiation on BIPVT panel surface, horizontal plane

The equations relating $S_{surface}$, $S_{horizontal}$ and $S_{incident}$ are:

$$S_{horizontal} = S_{incident} \sin \alpha$$

$$S_{surface} = S_{incident} \sin(\alpha + \beta)$$

$$S_{surface} = \frac{S_{horizontal}}{\sin \alpha} \sin(\alpha + \beta)$$

Where, α is the solar altitude angle, β is the tilt angle of the module measured from the horizontal.

The tilt angle has a major impact on the solar radiation incident on a surface. The tilt angle in this case is the roof pitch which is assumed to be 26.6°. The hourly solar radiations on the BIPVT panel surface and air temperatures of the three locations in 2010 are shown in Appendix C, Appendix D, and Appendix E.

The results of annual energy generation and energy conversion efficiency by the BIPVT system is listed in Table 7.2. The values of solar energy irradiation and energy generation for one typical day each month are also shown from Figure 7.3 to Figure 7.5 below.

Table 7.2: Annual BIPVT system's energy generation and efficiency of the BIPVT system in the three locations without considering system degradation

	Phoenix	**Albany**	**Duluth**
Electricity (kWh)	6404.4	3656.6	4835.7
Heat energy (kWh)	14740.7	4609.6	6750.4
Annual energy conversion efficiency	54.4%	35.6%	38.0%

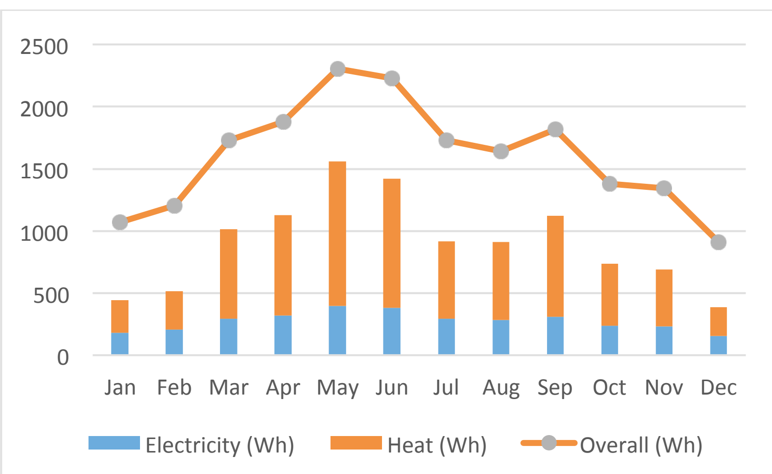

	Overall (Wh)	Electricity (Wh)	Heat (Wh)	Overall efficiency
Jan	1069.4	182.9	247.0	40.2%
Feb	1205.1	206.1	308.5	42.7%
Mar	1730.1	295.9	718.5	58.6%
Apr	1875.8	320.8	805.1	60.0%
May	2305.6	394.3	1167.5	67.7%
Jun	2226.2	380.7	1040.8	63.9%
Jul	1727.4	295.4	619.5	53.0%
Aug	1642.9	280.9	632.0	55.6%
Sep	1815.2	310.4	813.8	61.9%
Oct	1378.2	235.7	500.3	53.4%
Nov	1342.6	229.6	462.7	51.6%
Dec	909.3	155.5	232.0	42.6%

Figure 7.3: One typical day one 60cmX60cm (2'X2') BIPVT panel energy generation each month in Phoenix

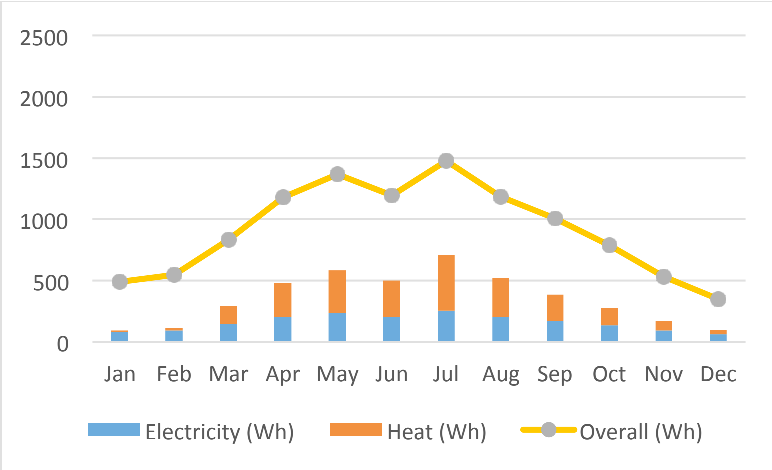

	Overall (Wh)	Electricity (Wh)	Heat (Wh)	Overall efficiency
Jan	488.2	83.5	0.0	17.1%
Feb	549.5	94.0	0.0	17.1%
Mar	836.2	143.0	75.2	26.1%
Apr	1181.7	202.1	250.8	38.3%
May	1369.5	234.2	347.4	42.5%
Jun	1195.2	204.4	295.9	41.9%
Jul	1478.0	252.7	455.2	47.9%
Aug	1184.9	202.6	319.8	44.1%
Sep	1007.8	172.3	215.7	38.5%
Oct	785.6	134.3	143.0	35.3%
Nov	531.8	90.9	20.1	20.9%
Dec	348.9	59.7	0.0	17.1%

Figure 7.4: One typical day one 60cmX60cm (2'X2') BIPVT panel energy generation each month in Albany

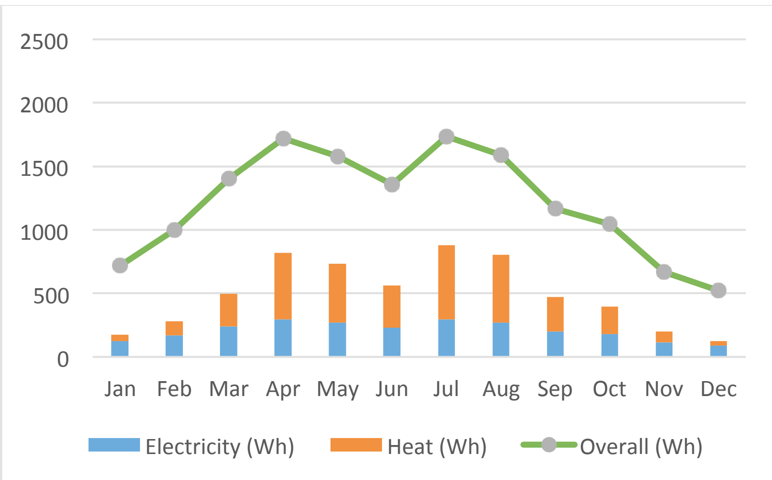

	Overall (Wh)	Electricity (Wh)	Heat (Wh)	Overall efficiency
Jan	719.0	122.9	0.0	17.1%
Feb	1002.4	171.4	72.7	24.4%
Mar	1405.7	240.4	114.1	25.2%
Apr	1718.8	293.9	326.0	36.1%
May	1580.0	270.2	438.9	44.9%
Jun	1359.0	232.4	328.5	41.3%
Jul	1735.5	296.8	581.9	50.6%
Aug	1589.3	271.8	530.4	50.5%
Sep	1168.4	199.8	270.9	40.3%
Oct	1044.0	178.5	117.9	28.4%
Nov	666.4	114.0	25.1	20.9%
Dec	520.7	89.0	0.0	17.1%

Figure 7.5: One typical day one 60cmX60cm (2'X2') BIPVT panel energy generation each month in Duluth

A typical performance ratio of PV system is 80%, since temperature effect has already been considered in our calculation, it is assumed as 90% in the study. Degradation of the panel is assumed to be 80% of the initial value at the end of the 25-year life time.

$$Life\ time\ energy\ generation = \sum_{n=1}^{LE} E_{annual} \times \frac{(LE-n)+DE(n-1)}{LE-1}$$

Where, LE is the life expectancy of the BIPVT system, 25 years, DE is the degradation of efficiency, 80%, E_{annual} is the typical annual energy generation without considering system degradation. The life cycle energy generation for each locations are listed in Table 7.3. The maximum efficiency of the three types of solar cell are estimated as 18%, 14%, and 12% respectively for Multi-Si, Mono-Si, and Ribbon Si.

Table 7.3: Life cycle energy generation without considering grid efficiency

	Phoenix			Albany			Duluth		
	Multi	Mono	Ribbon	Multi	Mono	Ribbon	Multi	Mono	Ribbon
Electricity (MWh)	144.1	113.8	96.9	82.3	65.0	55.3	108.8	85.9	73.2
Heat energy (MWh)	331.7			103.7			151.9		
Overall (MWh)	475.8	445.5	428.6	186	168.7	159	260.7	237.8	225.1

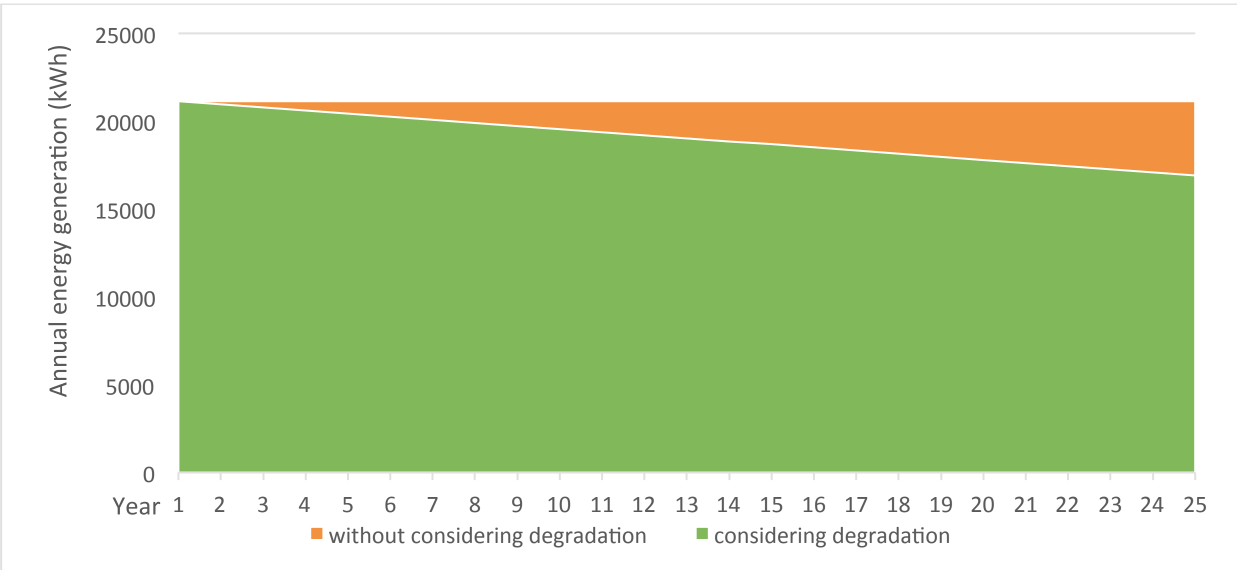

Figure 7.6: Life cycle energy generation with and without considering degradation in Phoenix (Multi-Si)

7.2. Use phase energy consumption

There are two components of the system that consume energy: the circulating pumps and the controller. The controller is assumed as 20W, and working 24/7. Each circulating pump is assumed to consume 200W when operating, regardless of water flow rate. The energy use in installation and M&O is estimated based the study of Agrawal and Tiwari [16].

Table 7.4: Installation and use phase energy consumption

Stage	Energy content	Phoenix	Albany	Duluth
Pump	200W/ea	1488kWh	1128kWh	1296kWh
Controller	20W	175.2kWh		
Installation	23.6-35kWh/m^2	732.5kWh		
M&O	1-2kWh/m^2/year	37.5kWh		

8. Results

ITe detailed results of the life cycle assessment are as follows: The GHG emission is estimated through the IPCC (Intergovernmental Panel on Climate Change) “GWP 2013 100a method”, in the form of CO_2 equivalent within an integrated 100-year time horizon. The energy use calculation uses the Cumulative Energy Demand method which evaluates non-renewable energy inputs only. All energy types are assumed to be provided by fossil fuels.

8.1. Global warming potential (GWP)

Figure 8.1 shows the life cycle GWP of the BIPVT system by considering lifetime expectation of different components. It shows clearly that the BIPVT panel contributes the most to GHG emission. The red dashes represent the alternative roof construction material the system can replace. However, the amount is very limited, thus not studied furthermore.

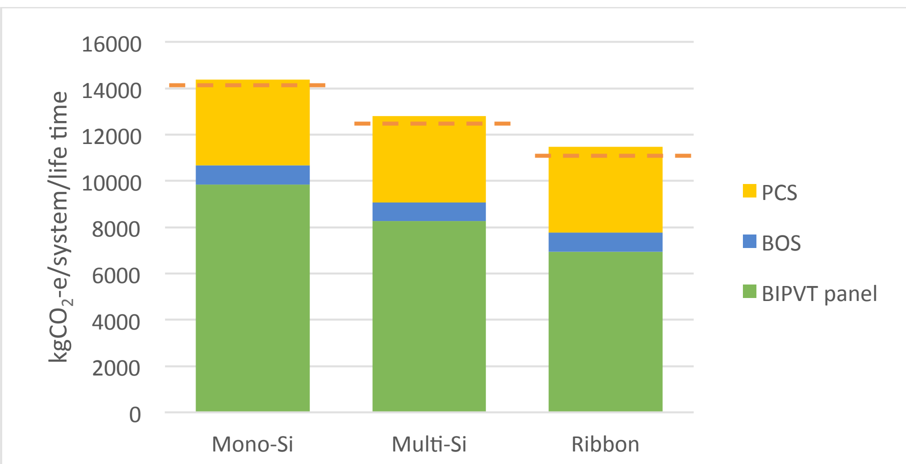

Figure 8.1: Life cycle GWP of the BIPVT system

The annual energy generation is expressed in terms of primary energy equivalent using the following equation below. Annual electricity is calculated by taking the ratio of the net electricity produced by the BIPVT system in one year to the life cycle energy efficiency of the current electric grid.

$$E_{out-eq,yr} = \frac{E_{agen}}{\eta_G} + E_{heat}$$

E_{agen}: Annual electricity generation

E_{heat}: Annual water heating energy generation

η_G: Grid efficiency, the average primary energy to electricity conversion efficiency at the demand side, which is taken as 0.33 here [32]

By dividing life cycle GWP and energy generation of the system, carbon footprint can be calculated. It is interpreted in the following figure in terms of three locations and three solar cell types. It is interesting that the emission factor of Duluth is less than that in Albany, although Duluth is much colder. Compare to the emission factor of various energy source (Figure 8.3), the studied BIPVT system actually performs very well with an emission factor of 19-43 gCO_2-e/kWh. However, if it is compared to other PV systems as shown in Figure 8.3, its GHG emission performance is not outstanding.

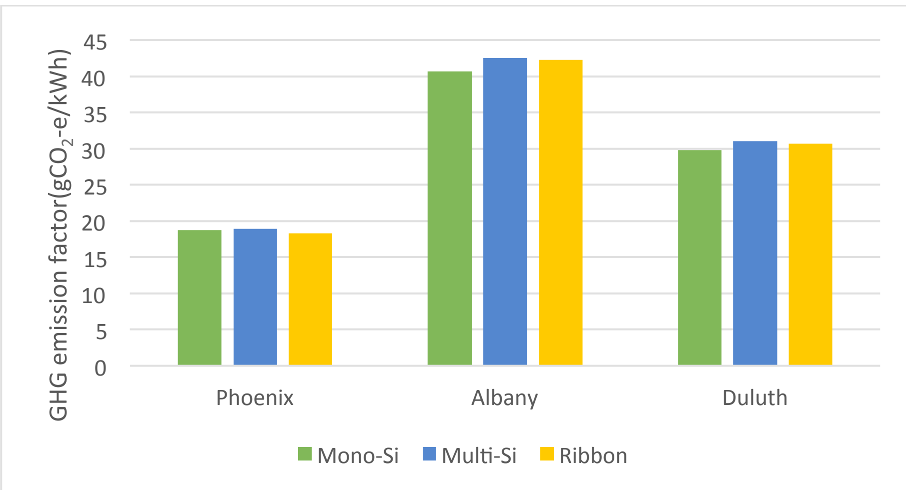

Figure 8.2: Life cycle GHG emission factors for the BIPVT system

Table 8.1: Life cycle emission factors for electricity generation[33]

Energy source	Hard coal	Lignite	Natural gas	Oil	Nuclear	Biomass	Hydropower	Solar energy	Wind
gCO_2-e/kWh	660-1050	800-1300	380-1000	530-900	3-35	8.5-130	2-20	13-190	3-41

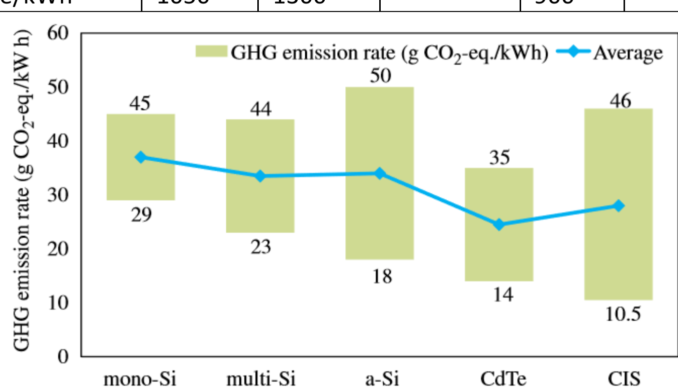

Figure 8.3: Review of GHG emission rates of PV electricity generated by various PV systems[34]

8.2. Cumulated energy demand (CED) & Energy payback time (EPBT)

The following figure shows the life cycle CED of the BIPVT system;2 again, the effect of the replaced material is not significant to the overall system.

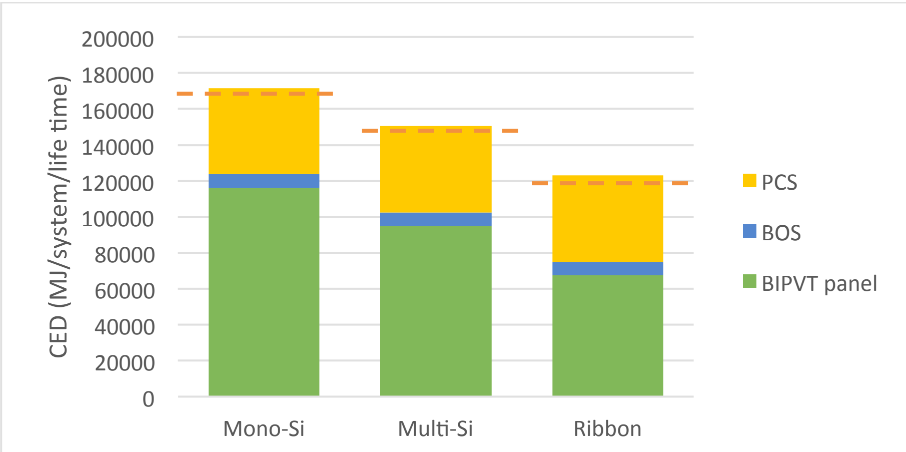

Figure 8.4: life cycle CED of the BIPVT system

Energy payback time is defined as the period required for a renewable energy system to generate the same amount of energy (in terms of primary energy equivalent) as was used to produce the system itself. The equation used for EPBT calculation is as follows:

$$\text{Energy payback time} = \frac{E_{mat} + E_{manuf} + E_{trans} + E_{inst}}{\frac{E_{agen}}{\eta_G} + E_{heat} - E_{M\&O}}$$

Where,

E_{mat}: Primary energy demand to produce materials comprising PV system

E_{manuf}: Primary energy demand to manufacture PV system

E_{trans}: Primary energy demand to transport materials used during the life cycle

E_{inst}: Primary energy demand to install the system

$E_{M\&O}$: Annual primary energy demand for operation and maintenance

Figure 8.5 shows the EPBT of the system, ~1.5 years in Phoenix, ~3.5 years in Albany, and ~2.5 years in Duluth. The system can be a great energy generation choice in terms of EPBT, especially for people in Phoenix and Duluth.

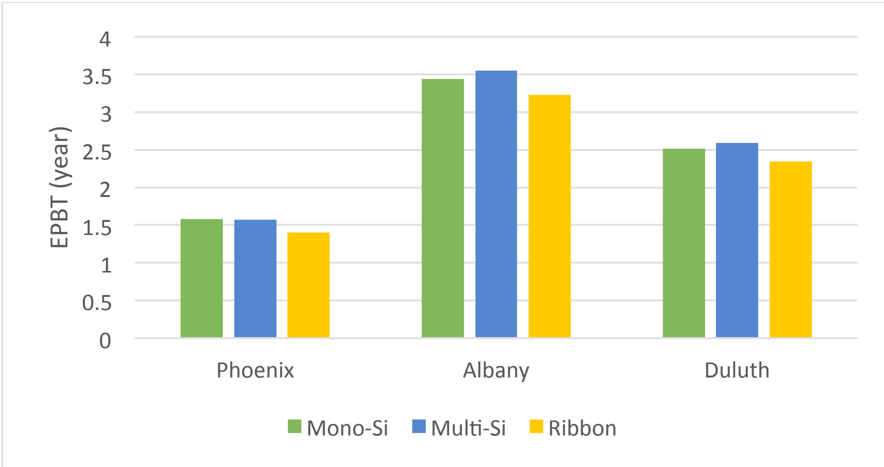

Figure 8.5: EPBT of the BIPVTs system

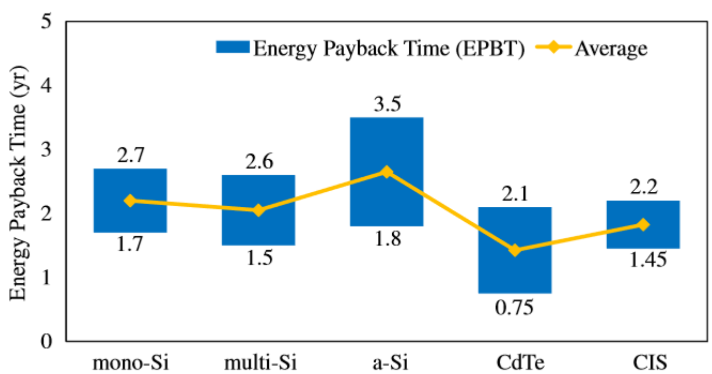

Figure 8.6: Review of energy payback time for various PV systems[34]

9. Conclusions & recommendations

The thesis provides a thorough life cycle inventory for estimating the environmental impact LCA of a recently developed BIPVT system, based on detailed and accurate component data. The primary findings indicate that the GHG emission factor and EPBT vary considerably between different climate zones, while the types of solar cells used have little effect. It is not surprising to see the performance of the system operating in Phoenix has great performance as this region has high insolation and hot weather all year round. It is interesting to see that the system operating in Duluth exhibits a better environmental performance than in Albany, although Albany is in a warmer climate zone. One reason is the higher annual solar radiation on the BIPVT panel surface in Duluth.

In comparison to some other PV systems, the BIPVT system's EPBT of 1.5 to 3.5 years has great potential for commercialization. With regard to the life cycle inventory, the solar cell contributes much more energy use and carbon emission than BOS and PCS combined. In PCS, water storage contributes most of the energy use and carbon emission.

Because the BIPVT system examined in this study is still in the laboratory phase, there are no actual operating data. Therefore, many assumptions made in this study were based on calculations, laboratory tests, and data from the literature.

REFERENCES

[1] "2011 Buildings Energy Data Book," 2011. [Online]. Available: http://buildingsdatabook.eren.doe.gov/ChapterIntro1.aspx. [Accessed: 07-Jul-2014].

[2] A. Kumar, P. Baredar, and U. Qureshi, "Historical and recent development of photovoltaic thermal (PVT) technologies," *Renew. Sustain. Energy Rev.*, vol. 42, pp. 1428–1436, Feb. 2015.

[3] P. G. Charalambous, G. G. Maidment, S. A. Kalogirou, and K. Yiakoumetti, "Photovoltaic thermal (PV/T) collectors: A review," *Appl. Therm. Eng.*, vol. 27, no. 2–3, pp. 275–286, Feb. 2007.

[4] S. A. Gevorgyan, M. Jørgensen, and F. C. Krebs, "A setup for studying stability and degradation of polymer solar cells," *Sol. Energy Mater. Sol. Cells*, vol. 92, no. 7, pp. 736–745, Jul. 2008.

[5] B. Sandnes and J. Rekstad, "A photovoltaic/thermal (PV/T) collector with a polymer absorber plate. Experimental study and analytical model," *Sol. Energy*, vol. 72, no. 1, pp. 63–73, Jan. 2002.

[6] S. A. Kalogirou, "Solar thermal collectors and applications," *Prog. Energy Combust. Sci.*, vol. 30, no. 3, pp. 231–295, 2004.

[7] H. M. Yin, D. J. Yang, G. Kelly, and J. Garant, "Design and performance of a novel building integrated PV/thermal system for energy efficiency of buildings," *Sol. Energy*, vol. 87, pp. 184–195, Jan. 2013.

[8] D. Yang and H. Yin, "Energy Conversion Efficiency of a Novel Hybrid Solar System for Photovoltaic, Thermoelectric, and Heat Utilization," *IEEE Trans. Energy Convers.*, vol. 26, no. 2, pp. 662–670, Jun. 2011.

[9] H. M. Yin, G. H. Paulino, W. G. Buttlar, and L. Z. Sun, "Effective Thermal Conductivity of Functionally Graded Particulate Nanocomposites With Interfacial Thermal Resistance," *J. Appl. Mech.*, vol. 75, no. 5, pp. 051113–051113, Jul. 2008.

[10] H. Kim, K. Cha, V. M. Fthenakis, P. Sinha, and T. Hur, "Life cycle assessment of cadmium telluride photovoltaic (CdTe PV) systems," *Sol. Energy*, vol. 103, pp. 78–88, May 2014.

[11] J.-Y. Lee, M.-S. Yu, K.-H. Cha, S.-Y. Lee, T. W. Lim, and T. Hur, "A study on the environmental aspects of hydrogen pathways in Korea," *Int. J. Hydrog. Energy*, vol. 34, no. 20, pp. 8455–8467, Oct. 2009.

[12] L. F. Cabeza, L. Rincón, V. Vilariño, G. Pérez, and A. Castell, "Life cycle assessment (LCA) and life cycle energy analysis (LCEA) of buildings and the building sector: A review," *Renew. Sustain. Energy Rev.*, vol. 29, pp. 394–416, Jan. 2014.

[13] V. M. Fthenakis and H. C. Kim, "Photovoltaics: Life-cycle analyses," *Sol. Energy*, vol. 85, no. 8, pp. 1609–1628, Aug. 2011.

[14] H. Kim, K. Cha, V. M. Fthenakis, P. Sinha, and T. Hur, "Life cycle assessment of cadmium telluride photovoltaic (CdTe PV) systems," *Sol. Energy*, vol. 103, pp. 78–88, May 2014.

[15] V. Fthenakis, R. Frischknecht, M. Raugei, H. C. Kim, E. Alsema, M. Held, and M. de Wild-Scholten, "Methodology guidelines on life cycle assessment of photovoltaic electricity," Nov. 2011.

[16] B. Agrawal and G. N. Tiwari, *Building Integrated Photovoltaic Thermal Systems*. The Royal Society of Chemistry, 2010.

[17] K. Kato, T. Hibino, K. Komoto, S. Ihara, S. Yamamoto, and H. Fujihara, "A life-cycle analysis on thin-film CdS/CdTe PV modules," *Sol. Energy Mater. Sol. Cells*, vol. 67, no. 1–4, pp. 279–287, Mar. 2001.

[18] "ecoinvent v3 | High-Quality LCI Database Integrated in SimaPro | PRé Sustainability." [Online]. Available: http://www.pre-sustainability.com/ecoinvent-high-quality-lci-database-integrated-in-simapro. [Accessed: 18-Jan-2015].

[19] L. Tong, X. Liu, X. Liu, Z. Yuan, and Q. Zhang, "Life cycle assessment of water reuse systems in an industrial park," *J. Environ. Manage.*, vol. 129, pp. 471–478, Nov. 2013.

[20] J.-Y. Lee, K.-H. Cha, T.-W. Lim, and T. Hur, "Eco-efficiency of H2 and fuel cell buses," *Int. J. Hydrog. Energy*, vol. 36, no. 2, pp. 1754–1765, Jan. 2011.

[21] Y. Fu, X. Liu, and Z. Yuan, "Life-cycle assessment of multi-crystalline photovoltaic (PV) systems in China," *J. Clean. Prod.*, vol. 86, pp. 180–190, Jan. 2015.

[22] E. A. A. M J De Wild-Scholten, "Environmental life cycle inventory of crystalline silicon photovoltaic module production," *MRS Proc.*, vol. 895, 2005.

[23] M. J. de W.-S. E. A. Alsema, "Environmental Impacts of Crystalline Silicon Photovoltaic Module Production," 2011.

[24] "State-Level Energy-Related Carbon Dioxide Emissions, 2000-2009." [Online]. Available: http://www.eia.gov/environment/emissions/state/analysis/. [Accessed: 18-Jan-2015].

[25] J. Li and Y. Chang, "Clean Production of Solar PV in China," *Greenpeace*. [Online]. Available: http://www.greenpeace.org/china/zh/publications/reports/climate-energy/2012/solar-clean-production/. [Accessed: 18-Dec-2014].

[26] H. Ye, W. Ma, B. Yang, J. Ren, D. Liu, and Y. Dai, "LCA study of metallurgical silicon process," *Light Met.*, Nov. 2007.

[27] V. Fthenakis, H. C. Kim, R. Frischknecht, M. Raugei, P. Sinha, and M. Stucki, "Life cycle inventories and life cycle assessment of photovoltaic systems," 2011.

[28] M. J. R. Perez, V. Fthenakis, H.-C. Kim, and A. O. Pereira, "Façade–integrated photovoltaics: a life cycle and performance assessment case study," *Prog. Photovolt. Res. Appl.*, vol. 20, no. 8, pp. 975–990, Dec. 2012.

[29] M. S. Buker, B. Mempouo, and S. B. Riffat, "Performance evaluation and techno-economic analysis of a novel building integrated PV/T roof collector: An experimental validation," *Energy Build.*, vol. 76, pp. 164–175, Jun. 2014.

[30] S. Wieder, *An Introduction to Solar Energy for Scientists and Engineers*. Krieger Publishing Company, 1992.

[31] B. Sopori, W. Chen, J. Madjdpour, and N. M. Ravindra, "Calculation of emissivity of Si wafers," *J. Electron. Mater.*, vol. 28, no. 12, pp. 1385–1389, Dec. 1999.

[32] M. Raugei, "Energy pay-back time: methodological caveats and future scenarios," *Prog. Photovolt. Res. Appl.*, vol. 21, no. 4, pp. 797–801, 2013.

[33] R. Turconi, A. Boldrin, and T. Astrup, "Life cycle assessment (LCA) of electricity generation technologies: Overview, comparability and limitations," *Renew. Sustain. Energy Rev.*, vol. 28, pp. 555–565, Dec. 2013.

[34] J. Peng, L. Lu, and H. Yang, "Review on life cycle assessment of energy payback and greenhouse gas emission of solar photovoltaic systems," *Renew. Sustain. Energy Rev.*, vol. 19, pp. 255–274, Mar. 2013.

Appendix A: Life cycle inventory data for the production of $1m^2$ mono-Si solar cell in our scope of study

Inventory name	Amount	Unit	Comment
Production of Mono-Si crystal from SoG-Si			
solar grade multi-Si	0.8401	kg	Companies that represent the current domain PV technologies in China
Silicon carbide	0.0094	kg	
quartz crucible	2.3392	kg	
argon	1.5980	kg	
hydrofluoric acid (49%)	0.0387	kg	
compressed air	2.8551	m3	
sodium hydroxide	0.0071	kg	
water	74.9492	kg	
electricity	23.9761	MJ	Clean Production of Solar PV in China[25]
steam	1.1566	kg	
Production of Mono-Si wafer from Mono-Si crystal			
quartz crucible	0.36	kg	for ingot growing
glass	0.01	kg	for temporarily attachment of bricks to wire sawing equipment, assumed same as multi wafers
steel wire	1.49	kg	for wafer cutting, assumed same as multi wafers
silicon carbide (SiC)	2.61	kg	for sawing slurry, assumed same as multi wafers
argon (Ar)	6.2	kg	for ingot growing
polyethylene glycol (PEG)	2.63	kg	for sawing slurry, assumed same as multi wafers
dipropylene glycol monomethyl ether (DPM)	0.3	kg	for sawing slurry, assumed same as multi wafers
adhesive	0.002	kg	for temporarily attachment of bricks to wire-sawing equipment
tenside (concentrated)	0.24	kg	for wafer cleaning
sodium hydroxide, 50% in H2O	0.015	kg	for wafer cleaning, assumed same as multi wafers
hydrochloric acid, 30% in H2O	0.0027	kg	for wafer cleaning, assumed same as multi wafers
acetic acid, 98% in H2O	0.039	kg	for wafer cleaning, assumed same as multi wafers
tap water	0.006	kg	for ingot sawing
water, deionized	65	kg	for wafer cleaning
electricity, medium voltage	145	kWh	total electricity consumption including direct and indirect process energy and overhead energy
natural gas	77	MJ	general use + furnaces
Production of Mono-Si solar cells from wafer			
water, cooling	1000	kg	cooling water
phosphorus paste	0.001455	kg	for emitter formation
metallization paste	0.075	kg	aggregated value for front and back pastes containing, silver content 1.6E-4 kg
polystyrene, expandable	0.000408	kg	for packaging

nitrogen (N_2)	1.852564	kg	
oxygen (O_2)	0.101923	kg	
argon (Ar)	0.025705	kg	
fluorinated compound mix (CF_4, C_2F_6, SF_6, NF_3)	0.00316	kg	aggregate value for different fluorinated source gases
ammoniac (NH_3)	0.006731	kg	for silicon nitride deposition
silane (SiH_4)	0.001212	kg	for silicon nitride deposition
sodium hydroxide, 50% in H_2O (NaOH)	0.157051	kg	
acetic acid, 98% in H_2O (CH_3COOH)	0.002833	kg	
hydrochloric acid, 30% in H_2O (HCl)	0.045641	kg	
hydrogen fluoride (HF) 100%	0.037756	kg	
nitric acid, 50% in H2O (HNO_3)	0.026731	kg	
POCl3 phosphoryl chloride	0.000217	kg	for emitter formation
phosphoric acid, industrial grade, 85% in H2O (H_3PO_4)	0.007628	kg	for emitter formation
sodium silicate	0.075	kg	
calcium chloride ($CaCl_2$)	0.021603	kg	
tetraisopropyltitanate (TPT, a titanium precursor)	1.42E-06	liter	for titanium dioxide antireflection coating deposition
isopropanol	0.078846	kg	
ethanol	0.00064	kg	
solvents, organic, unspecified	0.001436	kg	
water, deionized	137.8205	kg	
electricity, medium voltage	3.782051	kWh	
natural gas	4.75641	MJ	
fuel oil	0.032436	liter	

Appendix B: Section of roof structure provided by ESHA

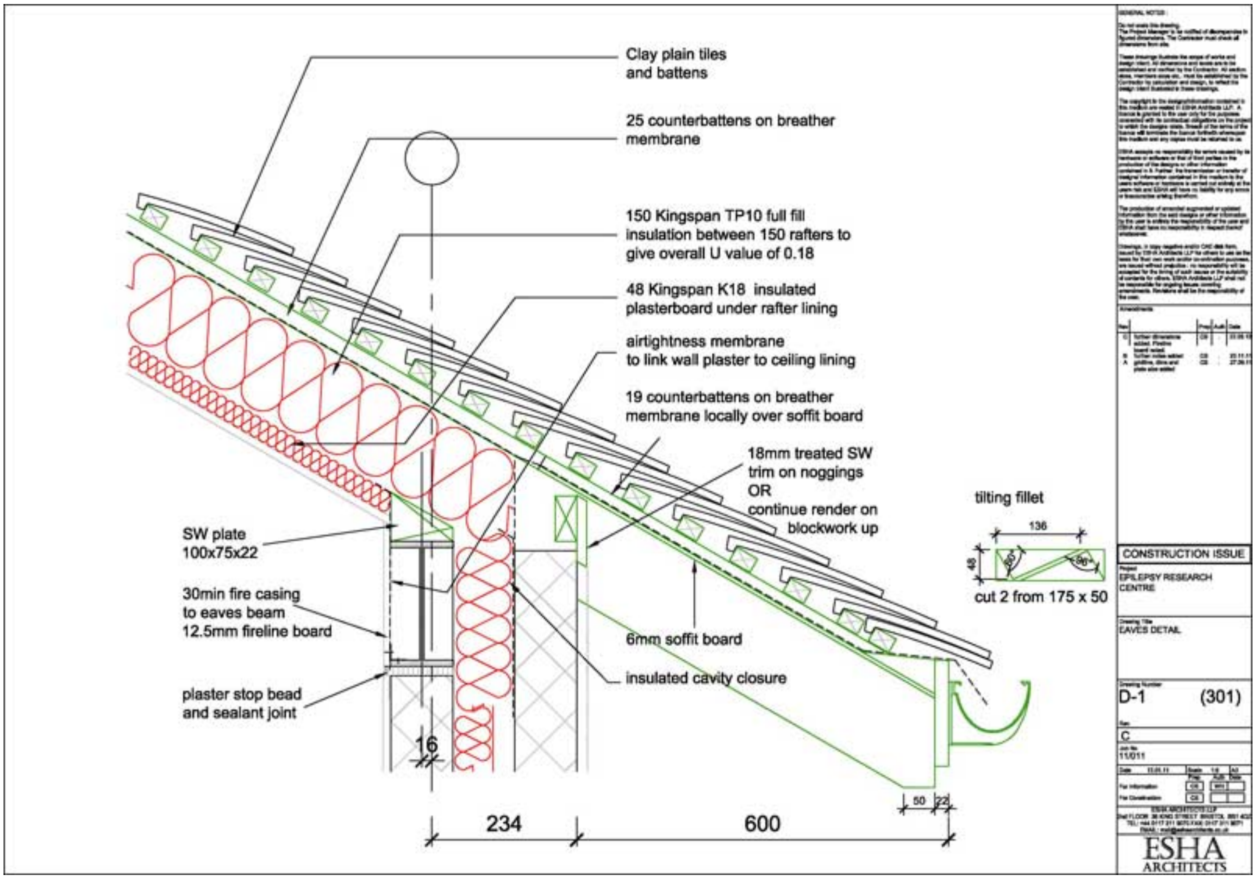

Appendix C: Hourly solar radiation (W/m^2) and air temperature (^{0}C) in Phoenix in 2010

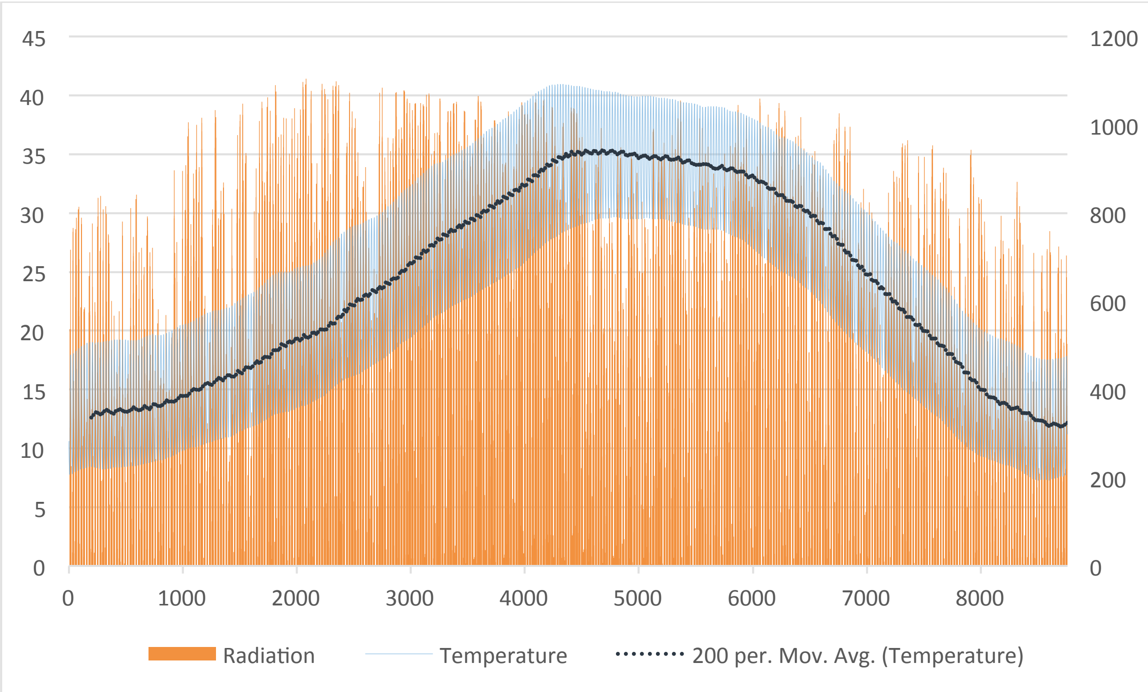

Appendix D: Hourly solar radiation (W/m^2) and air temperature (^{0}C) in Albany in 2010

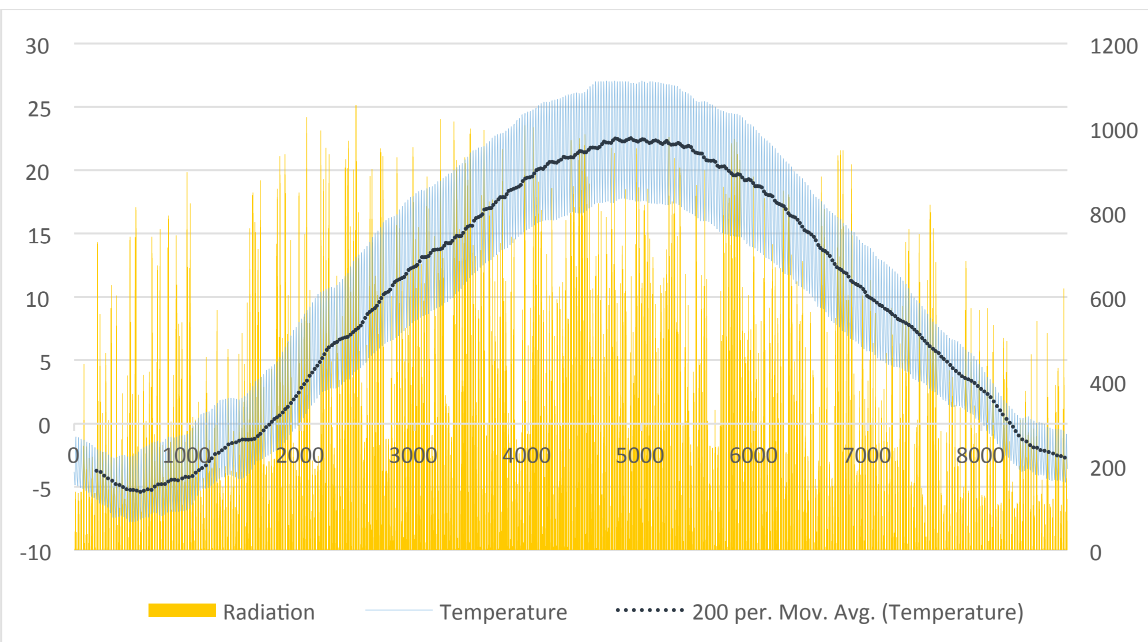

Appendix E: Hourly solar radiation (W/m2) and air temperature (^{0}C) in Duluth in 2010

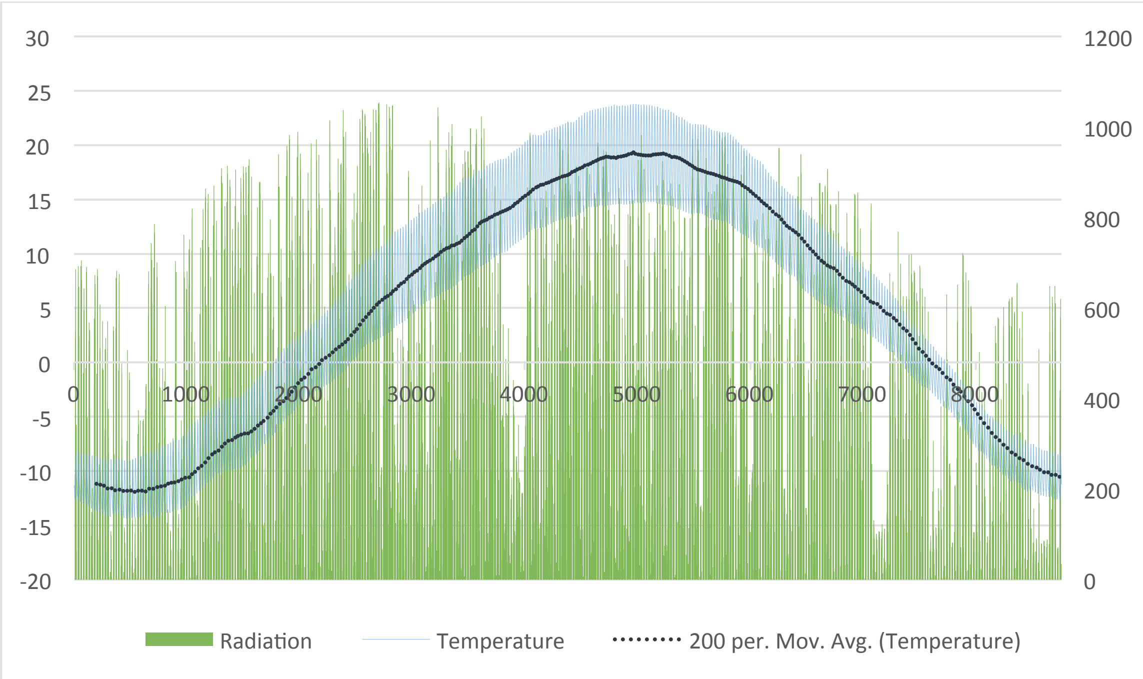

Appendix F: Energy generation calculation data in Phoenix (one typical day each month)

Month	Hour	Air temperatu	Irradiance	Electricity	Flow rate	Heat (Wh)
January	1:00	11.3924731	0	0		
	2:00	10.7043011	0	0		
	3:00	10.1218638	0	0		
	4:00	9.61648746	0	0		
	5:00	9.1953405	0	0		
	6:00	8.82795699	0	0		
	7:00	8.55913978	0	0		
	8:00	8.37275986	29.6839	1.26899		
	9:00	8.44982079	228.409	9.76448	10	12.54
	10:00	10.125448	409.387	17.5013	21	26.334
	11:00	12.3082437	552.852	23.6344	32	40.128
	12:00	14.3261649	580.577	24.8197	32	40.128
	13:00	15.9731183	591.601	25.2909	32	40.128
	14:00	17.2168459	606.489	25.9274	48	60.192
	15:00	18.1827957	521.396	22.2897	32	40.128
	16:00	18.8369176	399.227	17.0669		
	17:00	19.0394265	287.847	12.3054		
	18:00	18.6810036	70.1613	2.99939		
	19:00	17.3333333	0	0		
	20:00	15.8978495	0	0		
	21:00	14.6344086	0	0		
	22:00	13.6863799	0	0		
	23:00	12.8960573	0	0		
	0:00	12.155914	0	0		
			1069.41	182.869		259.578

Month	Hour	Air temperatu	Irradiance	Electricity	Flow rate	Heat (Wh)
February	1:00	13.4504	0	0		
	2:00	12.7123	0	0		
	3:00	12.04762	0	0		
	4:00	11.43849	0	0		
	5:00	10.88492	0	0		
	6:00	10.50595	0	0		
	7:00	10.23611	0	0		
	8:00	9.964286	85.8583	3.67044		
	9:00	10.40079	297.757	12.7291	10	12.54
	10:00	12.23611	482.603	20.6313	21	26.334
	11:00	14.37698	575.607	24.6072	32	40.128
	12:00	16.28968	578.299	24.7223	32	40.128
	13:00	17.90278	579.293	24.7648	32	40.128
	14:00	19.08929	592.227	25.3177	32	40.128
	15:00	2.00E+01	556.54	23.7921	36	45.144
	16:00	20.58135	509.817	21.7947	36	45.144
	17:00	20.81151	387.061	16.5469	15	18.81
	18:00	20.62302	165.677	7.08268		
	19:00	19.7877	9.73639	0.41623		
	20:00	18.44246	0	0		
	21:00	17.13294	0	0		
	22:00	16.09325	0	0		
	23:00	15.19246	0	0		
	0:00	14.37302	0	0		
			1205.12	206.075		308.484

Month	Hour	Air temperatu	Irradiance	Electricity	Flow rate	Heat (Wh)
March	1:00	16.2204	0	0		
	2:00	15.3548	0	0		
	3:00	14.5789	0	0		
	4:00	13.9086	0	0		
	5:00	13.328	0	0		
	6:00	12.8996	0	0		
	7:00	12.6649	27.5391	1.1773		
	8:00	13.4588	256.991	10.9864	10	12.54
	9:00	15.1882	503.101	21.5076	32	40.128
	10:00	17.2706	655.717	28.0319	48	60.192
	11:00	19.1882	792.286	33.8702	67	84.018
	12:00	20.8423	838.56	35.8484	91	114.114
	13:00	22.172	798.857	34.1512	72	90.288
	14:00	23.1452	819.78	35.0456	91	114.114
	15:00	23.8423	780.36	33.3604	72	90.288
	16:00	24.1703	625.574	26.7433	53	66.462
	17:00	24.1649	497.075	21.2499	25	31.35
	18:00	2.37E+01	277.409	11.8592	12	15.048
	19:00	22.7401	47.2382	2.01943		
	20:00	21.4552	0	0		
	21:00	20.1326	0	0		
	22:00	19.0824	0	0		
	23:00	18.1523	0	0		
	0:00	17.1989	0	0		
			1730.12	295.851		718.542

Month	Hour	Air temperatu	Irradiance	Electricity	Flow rate	Heat (Wh)
April	1:00	19.9944	0	0		
	2:00	19.0278	0	0		
	3:00	18.1889	0	0		
	4:00	17.3926	0	0		
	5:00	16.7556	0	0		
	6:00	16.2315	0.86166	0.03684		
	7:00	16.6981	137.118	5.86177		
	8:00	18.6167	384.221	16.4255	13	16.302
	9:00	20.9241	588.094	25.141	36	45.144
	10:00	22.9148	714.698	30.5533	72	90.288
	11:00	24.663	779.441	33.3211	72	90.288
	12:00	26.15	809.185	34.5926	91	114.114
	13:00	27.2907	844.054	36.0833	91	114.114
	14:00	28.1074	812.656	34.7411	91	114.114
	15:00	28.6185	777.18	33.2244	72	90.288
	16:00	28.7481	656.293	28.0565	53	66.462
	17:00	28.6204	559.313	23.9106	36	45.144
	18:00	28.0111	338.354	14.4646	15	18.81
	19:00	26.863	101.912	4.35672		
	20:00	25.5722	0	0		
	21:00	24.25	0	0		
	22:00	23.1407	0	0		
	23:00	22.1667	0	0		
	0:00	21.113	0	0		
			1875.84	320.769		805.068

Month	Hour	Air temperatu	Irradiance	Electricity	Flow rate	Heat (Wh)
May	1:00	25.276	0	0		
	2:00	24.2778	0	0		
	3:00	23.3154	0	0		
	4:00	22.4032	0	0		
	5:00	21.6452	0	0		
	6:00	21.1846	27.6389	1.18156		
	7:00	22.3172	276.036	11.8005	12	15.048
	8:00	24.3011	525.539	22.4668	36	45.144
	9:00	26.4409	718.631	30.7215	72	90.288
	10:00	28.4032	812.516	34.7351	91	114.114
	11:00	30.0806	914.423	39.0916	112	140.448
	12:00	31.4498	962.034	41.1269	112	140.448
	13:00	32.5824	958.496	40.9757	112	140.448
	14:00	33.457	958.888	40.9925	112	140.448
	15:00	33.948	884.721	37.8218	91	114.114
	16:00	34.1559	803.183	34.3361	91	114.114
	17:00	34.0323	667.569	28.5386	53	66.462
	18:00	33.5	482.014	20.6061	25	31.35
	19:00	32.4857	216.566	9.2582	12	15.048
	20:00	31.147	14.2734	0.61019		
	21:00	29.7222	0	0		
	22:00	28.4964	0	0		
	23:00	27.4892	0	0		
	0:00	26.4821	0	0		
			2305.63	394.263		1167.47

Month	Hour	Air temperatu	Irradiance	Electricity	Flow rate	Heat (Wh)
June	1:00	29.9315	0	0		
	2:00	28.9111	0	0		
	3:00	27.8944	0	0		
	4:00	26.9426	0	0		
	5:00	26.1778	0	0		
	6:00	25.813	37.7454	1.61361		
	7:00	27.0315	275.498	11.7775	12	15.048
	8:00	28.9944	514.117	21.9785	36	45.144
	9:00	31.1222	691.453	29.5596	53	66.462
	10:00	33.0556	765.801	32.738	72	90.288
	11:00	34.7796	847.331	36.2234	91	114.114
	12:00	36.2222	903.586	38.6283	112	140.448
	13:00	37.4019	879.282	37.5893	91	114.114
	14:00	38.3037	898.946	38.43	91	114.114
	15:00	38.887	864.252	36.9468	91	114.114
	16:00	39.1685	805.889	34.4518	91	114.114
	17:00	39.0852	670.253	28.6533	53	66.462
	18:00	38.6352	459.822	19.6574	25	31.35
	19:00	37.713	256.284	10.9562	12	15.048
	20:00	36.2519	34.5667	1.47772		
	21:00	34.6444	0	0		
	22:00	33.2074	0	0		
	23:00	32.1889	0	0		
	0:00	31.1537	0	0		
			2226.21	380.681		1040.82

Month	Hour	Air temperatu	Irradiance	Electricity	Flow rate	Heat (Wh)
July	1:00	32.3136201	0	0		
	2:00	31.5896057	0	0		
	3:00	30.8978495	0	0		
	4:00	30.2293907	0	0		
	5:00	29.7096774	0	0		
	6:00	29.3243728	18.6751	0.79836		
	7:00	30.0537634	164.355	7.02616		
	8:00	31.4677419	329.901	14.1033	15	18.81
	9:00	33.1451613	516.311	22.0723	36	45.144
	10:00	34.7043011	606.337	25.9209	53	66.462
	11:00	36.1738351	674.232	28.8234	53	66.462
	12:00	37.4480287	686.735	29.3579	53	66.462
	13:00	38.5555556	725.163	31.0007	72	90.288
	14:00	39.4605735	728.283	31.1341	72	90.288
	15:00	40.0698925	696.12	29.7591	53	66.462
	16:00	40.3422939	599.019	25.6081	36	45.144
	17:00	40.3100358	585.979	25.0506	36	45.144
	18:00	39.8315412	357.841	15.2977	15	18.81
	19:00	38.8315412	191.918	8.20452		
	20:00	37.5	28.7835	1.2305		
	21:00	36.2150538	0	0		
	22:00	34.9910394	0	0		
	23:00	34.0734767	0	0		
	0:00	33.1648746	0	0		
			1727.41	295.388		619.476

Month	Hour	Air temperatu	Irradiance	Electricity	Flow rate	Heat (Wh)
August	1:00	31.5914	0	0		
	2:00	30.95161	0	0		
	3:00	30.31183	0	0		
	4:00	29.78674	0	0		
	5:00	29.31541	0	0		
	6:00	28.94265	1.9876	0.08497		
	7:00	29.31183	105.794	4.52269		
	8:00	30.60753	311.446	13.3143	15	18.81
	9:00	32.24731	470.981	20.1344	25	31.35
	10:00	33.80824	578.465	24.7294	36	45.144
	11:00	35.25986	611.996	26.1628	53	66.462
	12:00	36.53047	742.75	31.7526	72	90.288
	13:00	37.66129	739.516	31.6143	72	90.288
	14:00	38.51971	700.285	29.9372	72	90.288
	15:00	39.10753	737.464	31.5266	72	90.288
	16:00	39.319	597.868	25.5589	36	45.144
	17:00	39.23297	525.34	22.4583	36	45.144
	18:00	38.67204	320.095	13.6841	15	18.81
	19:00	37.50358	124.943	5.34132		
	20:00	36.19355	2.80383	0.11986		
	21:00	34.9086	0	0		
	22:00	33.84767	0	0		
	23:00	33.05197	0	0		
	0:00	32.2509	0	0		
			1642.93	280.942		632.016

Month	Hour	Air temperatu	Irradiance	Electricity	Flow rate	Heat (Wh)
Septemb	1:00	28.5259	0	0		
	2:00	27.7796	0	0		
	3:00	27.1037	0	0		
	4:00	26.5185	0	0		
	5:00	26.05	0	0		
	6:00	25.6185	0	0		
	7:00	25.7593	88.3085	3.77519		
	8:00	27.3241	347.563	14.8583	15	18.81
	9:00	29.3296	581.828	24.8732	36	45.144
	10:00	31.213	734.334	31.3928	72	90.288
	11:00	32.8574	834.825	35.6887	91	114.114
	12:00	34.2815	814.896	34.8368	91	114.114
	13:00	35.3722	829.807	35.4743	91	114.114
	14:00	36.2241	818.562	34.9935	91	114.114
	15:00	36.6981	771.046	32.9622	72	90.288
	16:00	36.8074	617.786	26.4103	53	66.462
	17:00	36.4556	496.468	21.224	25	31.35
	18:00	35.6722	280.61	11.9961	12	15.048
	19:00	34.3741	44.8847	1.91882		
	20:00	33.0907	0	0		
	21:00	31.8926	0	0		
	22:00	30.9148	0	0		
	23:00	30.0574	0	0		
	0:00	29.2019	0	0		
			1815.23	310.404		813.846

Month	Hour	Air temperatu	Irradiance	Electricity	Flow rate	Heat (Wh)
October	1:00	21.7975	0	0		
	2:00	21.0681	0	0		
	3:00	20.4014	0	0		
	4:00	19.8315	0	0		
	5:00	19.3943	0	0		
	6:00	19.0358	0	0		
	7:00	18.9373	29.6379	1.26702		
	8:00	20.4498	257.107	10.9913	12	15.048
	9:00	22.7545	437.501	18.7032	25	31.35
	10:00	24.9229	586.719	25.0822	36	45.144
	11:00	26.7563	709.865	30.3467	72	90.288
	12:00	28.2276	670.479	28.663	53	66.462
	13:00	29.3584	719.16	30.7441	72	90.288
	14:00	30.2312	652.905	27.9117	53	66.462
	15:00	30.7043	546.887	23.3794	36	45.144
	16:00	30.6971	477.167	20.3989	25	31.35
	17:00	30.2348	325.157	13.9004	15	18.81
	18:00	29.0412	99.4049	4.24956		
	19:00	27.5287	0.97279	0.04159		
	20:00	26.1344	0	0		
	21:00	25.043	0	0		
	22:00	24.1362	0	0		
	23:00	23.2079	0	0		
	0:00	22.3208	0	0		
			1378.24	235.679		500.346

Month	Hour	Air temperatu	Irradiance	Electricity	Flow rate	Heat (Wh)
Novembe	1:00	14.8389	0	0		
	2:00	14.187	0	0		
	3:00	13.5907	0	0		
	4:00	13.1019	0	0		
	5:00	12.7352	0	0		
	6:00	12.463	0	0		
	7:00	12.2481	5.86852	0.25088		
	8:00	13.1185	175.492	7.50228		
	9:00	15.3537	427.892	18.2924	21	26.334
	10:00	17.6204	561.983	24.0248	32	40.128
	11:00	19.5648	690.076	29.5007	48	60.192
	12:00	21.1185	694.142	29.6746	53	66.462
	13:00	22.2796	715.505	30.5879	72	90.288
	14:00	23.1481	695.484	29.7319	53	66.462
	15:00	23.6537	604.707	25.8512	53	66.462
	16:00	23.663	477.753	20.4239	25	31.35
	17:00	23.0574	283.556	12.122	12	15.048
	18:00	21.4741	38.0829	1.62804		
	19:00	19.9704	0	0		
	20:00	18.7352	0	0		
	21:00	17.7352	0	0		
	22:00	16.9019	0	0		
	23:00	16.1389	0	0		
	0:00	15.3389	0	0		
			1342.64	229.591		462.726

Month	Hour	Air temperatu	Irradiance	Electricity	Flow rate	Heat (Wh)
Decembe	1:00	10.2778	0	0		
	2:00	9.72401	0	0		
	3:00	9.2509	0	0		
	4:00	8.82796	0	0		
	5:00	8.48566	0	0		
	6:00	8.23118	0	0		
	7:00	8.06093	0	0		
	8:00	8.29211	47.4331	2.02777		
	9:00	10.0054	223.978	9.57507	10	12.54
	10:00	12.1219	371.694	15.8899	13	16.302
	11:00	14.1111	505.695	21.6184	32	40.128
	12:00	15.6667	508.078	21.7204	32	40.128
	13:00	16.8871	534.9	22.867	32	40.128
	14:00	17.7832	501.997	21.4604	32	40.128
	15:00	18.3315	418.83	17.905	21	26.334
	16:00	18.414	324.585	13.876	13	16.302
	17:00	17.8136	182.873	7.81784		
	18:00	16.2384	17.2868	0.73901		
	19:00	14.9158	0	0		
	20:00	13.8172	0	0		
	21:00	12.9588	0	0		
	22:00	12.2366	0	0		
	23:00	11.5376	0	0		
	0:00	10.8871	0	0		
			909.338	155.497		231.99

Appendix G: Energy generation calculation data in Albany (one typical day each month)

Month	Hour	Air temperatu	Irradiance	Electricity	Flow rate (	Heat (Wh)
January	1:00	-5.43	0	0		
	2:00	-5.72	0	0		
	3:00	-5.87	0	0		
	4:00	-6.06	0	0		
	5:00	-6.26	0	0		
	6:00	-6.42	0	0		
	7:00	-6.57	0	0		
	8:00	-6.67	22.8	0.9747		
	9:00	-6.62	116.15	4.96541		
	10:00	-5.78	215.75	9.22331		
	11:00	-4.82	266.33	11.3856		
	12:00	-3.81	287.35	12.2842		
	13:00	-3.06	314.08	13.4269	10	9.05667
	14:00	-2.51	296.99	12.6963		
	15:00	-2.08	228.92	9.78633		
	16:00	-2.01	162.69	6.955		
	17:00	-2.27	41.86	1.78952		
	18:00	-2.86	0	0		
	19:00	-3.48	0	0		
	20:00	-3.98	0	0		
	21:00	-4.37	0	0		
	22:00	-4.68	0	0		
	23:00	-4.96	0	0		
	0:00	-5.15	0	0		
			488.23	83.4873		9.05667

Month	Hour	Air temperatu	Irradiance	Electricity	Flow rate (	Heat (Wh)
February	1:00	-4.0734	0	0		
	2:00	-4.4147	0	0		
	3:00	-4.6567	0	0		
	4:00	-4.9683	0	0		
	5:00	-5.1488	0	0		
	6:00	-5.3849	0	0		
	7:00	-5.5675	0.5	0.02138		
	8:00	-5.7698	46.7595	1.99897		
	9:00	-5.252	146.247	6.25207		
	10:00	-4.1389	251.125	10.7356		
	11:00	-3.0556	288.039	12.3136		
	12:00	-2.0417	319.859	13.674	10	9.05667
	13:00	-1.1508	321.544	13.746	10	9.05667
	14:00	-0.4246	299.379	12.7985		
	15:00	8.72E-17	238.069	10.1774		
	16:00	0.25198	190.146	8.12873		
	17:00	0.15476	89.7433	3.83653		
	18:00	-0.375	6.70981	0.28684		
	19:00	-1.2361	0	0		
	20:00	-1.9028	0	0		
	21:00	-2.4722	0	0		
	22:00	-2.9663	0	0		
	23:00	-3.3413	0	0		
	0:00	-3.6746	0	0		
			549.53	93.9696		18.1133

Month	Hour	Air temperatu	Irradiance	Electricity	Flow rate (	Heat (Wh)
March	1:00	-0.1738	0	0		
	2:00	-0.4749	0	0		
	3:00	-0.8333	0	0		
	4:00	-1.1756	0	0		
	5:00	-1.3853	0	0		
	6:00	-1.6201	0.97838	0.04183		
	7:00	-1.4158	41.0614	1.75538		
	8:00	-0.5842	164.801	7.04522		
	9:00	0.61111	267.533	11.4371	10	12.54
	10:00	1.70609	384.318	16.4296	13	16.302
	11:00	2.77778	430.241	18.3928	20	25.08
	12:00	3.76344	408.257	17.453	20	25.08
	13:00	4.5448	469.81	20.0844	20	25.08
	14:00	5.08065	368.891	15.7701	13	16.302
	15:00	5.39247	318.193	13.6027	13	16.302
	16:00	5.45341	285.068	12.1867	10	12.54
	17:00	5.14875	149.464	6.38961		
	18:00	4.4086	54.3255	2.32241		
	19:00	3.39964	1.8561	0.07935		
	20:00	2.55018	0	0		
	21:00	1.89785	0	0		
	22:00	1.34588	0	0		
	23:00	0.8853	0	0		
	0:00	0.45878	0	0		
			836.2	142.99		149.226

Month	Hour	Air temperatu	Irradiance	Electricity	Flow rate (	Heat (Wh)
April	1:00	6.11667	0	0		
	2:00	5.65185	0	0		
	3:00	5.23333	0	0		
	4:00	4.85741	0	0		
	5:00	4.5	0	0		
	6:00	4.66111	41.8914	1.79086		
	7:00	6.05	182.106	7.78504		
	8:00	7.42037	284.737	12.1725	10	12.54
	9:00	8.74259	356.658	15.2471	13	16.302
	10:00	9.9537	483.387	20.6648	20	25.08
	11:00	11.1037	505.686	21.6181	32	40.128
	12:00	12.0741	515.734	22.0476	32	40.128
	13:00	12.7296	535.583	22.8962	32	40.128
	14:00	13.2537	519.115	22.1922	32	40.128
	15:00	13.4241	439.737	18.7987	21	26.334
	16:00	13.2648	407.321	17.413	21	26.334
	17:00	12.8981	262.826	11.2358	10	12.54
	18:00	11.9481	158.215	6.7637		
	19:00	10.7111	33.9066	1.44951		
	20:00	9.61111	0	0		
	21:00	8.77593	0	0		
	22:00	8.03889	0	0		
	23:00	7.40556	0	0		
	0:00	6.78889	0	0		
			1181.73	202.075		279.642

Month	Hour	Air temperatu	Irradiance	Electricity	Flow rate (	Heat (Wh)
May	1:00	11.3799	0	0		
	2:00	10.7921	0	0		
	3:00	10.3208	0	0		
	4:00	9.87814	0	0		
	5:00	9.62007	9.6671	0.41327		
	6:00	10.6254	112.189	4.79608		
	7:00	12.1846	258.409	11.047	10	12.54
	8:00	13.552	404.597	17.2965	21	26.334
	9:00	14.9194	420.407	17.9724	21	26.334
	10:00	16.2007	562.691	24.055	32	40.128
	11:00	17.3961	507.357	21.6895	32	40.128
	12:00	18.3136	566.223	24.206	32	40.128
	13:00	18.9391	595.692	25.4658	32	40.128
	14:00	19.3763	523.188	22.3663	32	40.128
	15:00	19.5502	466.313	19.9349	21	26.334
	16:00	19.3656	435.614	18.6225	21	26.334
	17:00	18.9355	313.999	13.4234	13	16.302
	18:00	18.043	213.519	9.12795	10	12.54
	19:00	16.8405	85.3495	3.64869		
	20:00	15.4337	2.92082	0.12486		
	21:00	14.4337	0	0		
	22:00	13.5968	0	0		
	23:00	12.8387	0	0		
	0:00	12.1505	0	0		
			1369.53	234.19		347.358

Month	Hour	Air temperatu	Irradiance	Electricity	Flow rate (	Heat (Wh)
June	1:00	16.287	0	0		
	2:00	15.7833	0	0		
	3:00	15.3648	0	0		
	4:00	15.0296	0	0		
	5:00	14.887	14.5883	0.62365		
	6:00	16.0611	108.854	4.65349		
	7:00	17.4093	217.429	9.29508	10	12.54
	8:00	18.6926	287.462	12.289	10	12.54
	9:00	19.9852	372.136	15.9088	13	16.302
	10:00	21.2278	475.583	20.3312	25	31.35
	11:00	22.3296	452.232	19.3329	25	31.35
	12:00	23.1963	440.585	18.835	25	31.35
	13:00	23.7722	551.168	23.5625	36	45.144
	14:00	24.1222	389.236	16.6399	15	18.81
	15:00	24.2704	409.466	17.5047	25	31.35
	16:00	24.1778	418.808	17.9041	25	31.35
	17:00	23.763	305.153	13.0453	15	18.81
	18:00	22.9241	217.617	9.30311	12	15.048
	19:00	21.7574	111.191	4.7534		
	20:00	20.213	9.27591	0.39655		
	21:00	19.1759	0	0		
	22:00	18.3222	0	0		
	23:00	17.6259	0	0		
	0:00	17.0222	0	0		
			1195.2	204.379		295.944

Month	Hour	Air temperatu	Irradiance	Electricity	Flow rate (	Heat (Wh)
July	1:00	18.765233	0	0		
	2:00	18.2616487	0	0		
	3:00	17.8835125	0	0		
	4:00	17.4677419	0	0		
	5:00	17.2956989	8.410058	0.35953		
	6:00	18.2885305	111.8083	4.7798		
	7:00	19.7455197	278.4042	11.9018	10	12.54
	8:00	21.125448	362.6646	15.5039	15	18.81
	9:00	22.4982079	470.5096	20.1143	25	31.35
	10:00	23.7831541	621.0271	26.5489	53	66.462
	11:00	24.9139785	565.0146	24.1544	36	45.144
	12:00	25.7616487	536.1716	22.9213	36	45.144
	13:00	26.3924731	605.2071	25.8726	53	66.462
	14:00	26.7060932	558.2578	23.8655	36	45.144
	15:00	26.702509	538.612	23.0257	36	45.144
	16:00	26.4713262	506.5666	21.6557	36	45.144
	17:00	25.9982079	371.1318	15.8659	15	18.81
	18:00	25.2329749	245.0296	10.475	12	15.048
	19:00	24.0322581	122.5328	5.23828		
	20:00	22.546595	10.5377	0.45049		
	21:00	21.4498208	0	0		
	22:00	20.6630824	0	0		
	23:00	19.9677419	0	0		
	0:00	19.3405018	0	0		
			1477.971	252.733		455.202

Month	Hour	Air temperatu	Irradiance	Electricity	Flow rate (	Heat (Wh)
August	1:00	17.8513	0	0		
	2:00	17.3746	0	0		
	3:00	17.0215	0	0		
	4:00	16.6864	0	0		
	5:00	16.3853	0	0		
	6:00	16.7616	36.1042	1.54345		
	7:00	18.2079	169.247	7.23532		
	8:00	19.6362	280.043	11.9719	10	12.54
	9:00	21.1129	405.182	17.3215	25	31.35
	10:00	22.5143	486.787	20.8102	25	31.35
	11:00	23.6953	520.307	22.2431	36	45.144
	12:00	24.647	515.67	22.0449	36	45.144
	13:00	25.2634	529.071	22.6178	36	45.144
	14:00	25.6685	484.011	20.6915	25	31.35
	15:00	25.7832	437.191	18.6899	25	31.35
	16:00	25.5215	409.908	17.5236	25	31.35
	17:00	24.9642	273.05	11.6729	12	15.048
	18:00	24.0179	155.48	6.64677		
	19:00	22.3656	37.6668	1.61025		
	20:00	21.0502	0.03226	0.00138		
	21:00	20.1398	0	0		
	22:00	19.4247	0	0		
	23:00	18.853	0	0		
	0:00	18.3172	0	0		
			1184.94	202.624		319.77

Month	Hour	Air temperatu	Irradiance	Electricity	Flow rate (	Heat (Wh)
Septembe	1:00	13.8963	0	0		
	2:00	13.5056	0	0		
	3:00	13.1889	0	0		
	4:00	12.8537	0	0		
	5:00	12.5852	0	0		
	6:00	12.4815	17.3911	0.74347		
	7:00	13.6037	144.657	6.18407		
	8:00	15.1167	282.301	12.0684	10	12.54
	9:00	16.5722	353.949	15.1313	13	16.302
	10:00	17.9333	461.4	19.7248	21	26.334
	11:00	19.2241	472.82	20.213	21	26.334
	12:00	20.2315	435.364	18.6118	25	31.35
	13:00	20.9222	468.078	20.0103	25	31.35
	14:00	21.3352	389.991	16.6721	15	18.81
	15:00	21.4204	361.158	15.4395	15	18.81
	16:00	21.1296	324.963	13.8922	15	18.81
	17:00	20.3722	219.538	9.38524	12	15.048
	18:00	18.9333	93.8572	4.0124		
	19:00	17.4574	5.91492	0.25286		
	20:00	16.4741	0	0		
	21:00	15.7722	0	0		
	22:00	15.1574	0	0		
	23:00	14.6074	0	0		
	0:00	14.0889	0	0		
			1007.85	172.342		215.688

Month	Hour	Air temperatu	Irradiance	Electricity	Flow rate (	Heat (Wh)
October	1:00	7.77061	0	0		
	2:00	7.42294	0	0		
	3:00	7.12007	0	0		
	4:00	6.85842	0	0		
	5:00	6.6362	0	0		
	6:00	6.48387	0	0		
	7:00	6.8172	58.1849	2.4874		
	8:00	8.3871	175.349	7.49617		
	9:00	9.7957	264.688	11.3154	10	12.54
	10:00	11.1864	351.292	15.0177	13	16.302
	11:00	12.4444	360.233	15.4	13	16.302
	12:00	13.4122	420.79	17.9888	21	26.334
	13:00	14.1631	438.192	18.7327	21	26.334
	14:00	14.5179	374.802	16.0228	13	16.302
	15:00	14.595	327.221	13.9887	13	16.302
	16:00	14.1738	249.77	10.6776	10	12.54
	17:00	13.1129	109.383	4.6761		
	18:00	11.6111	12.4477	0.53214		
	19:00	10.6756	0	0		
	20:00	9.96595	0	0		
	21:00	9.34946	0	0		
	22:00	8.88351	0	0		
	23:00	8.41219	0	0		
	0:00	7.99462	0	0		
			785.588	134.336		142.956

Month	Hour	Air temperatu	Irradiance	Electricity	Flow rate (	Heat (Wh)
Novembe	1:00	3.14815	0	0		
	2:00	2.9537	0	0		
	3:00	2.69259	0	0		
	4:00	2.50556	0	0		
	5:00	2.37407	0	0		
	6:00	2.22963	0	0		
	7:00	2.16852	5.1935	0.22202		
	8:00	2.87963	67.4985	2.88556		
	9:00	3.96852	172.051	7.35519		
	10:00	5.07593	282.524	12.0779	10	12.54
	11:00	6.02407	288.266	12.3234	10	12.54
	12:00	6.83148	314.845	13.4596	13	16.302
	13:00	7.37593	342.957	14.6614	13	16.302
	14:00	7.58704	270.284	11.5547	10	12.54
	15:00	7.56111	214.578	9.17321	10	12.54
	16:00	7.04259	147.162	6.2912		
	17:00	6.17593	21.8747	0.93514		
	18:00	5.37407	0	0		
	19:00	4.88889	0	0		
	20:00	4.44074	0	0		
	21:00	4.13519	0	0		
	22:00	3.81481	0	0		
	23:00	3.54444	0	0		
	0:00	3.31481	0	0		
			531.809	90.9393		82.764

Month	Hour	Air temperatu	Irradiance	Electricity	Flow rate (	Heat (Wh)
Decembe	1:00	-2.3513	0	0		
	2:00	-2.5233	0	0		
	3:00	-2.6846	0	0		
	4:00	-2.871	0	0		
	5:00	-3.0358	0	0		
	6:00	-3.1416	0	0		
	7:00	-3.1685	0	0		
	8:00	-2.9928	18.6877	0.7989		
	9:00	-2.2294	99.1906	4.2404		
	10:00	-1.3369	167.716	7.16985		
	11:00	-0.586	194.25	8.3042		
	12:00	0.13082	228.748	9.77897	10	12.54
	13:00	0.58961	235.42	10.0642	10	12.54
	14:00	0.9086	219.344	9.37696	10	12.54
	15:00	0.85663	147.552	6.30786		
	16:00	0.44086	79.7601	3.40975		
	17:00	-0.2563	5.02679	0.2149		
	18:00	-0.7222	0	0		
	19:00	-1.0753	0	0		
	20:00	-1.3566	0	0		
	21:00	-1.6219	0	0		
	22:00	-1.8961	0	0		
	23:00	-2.1434	0	0		
	0:00	-2.3333	0	0		
			348.924	59.666		37.62

Appendix H: Energy generation calculation data in Duluth (one typical day each month)

		Air temperatu	Irradiance (	Electricity	Flow rate	Heat (Wh)
January	1:00	-11.951613	0	0		
	2:00	-12.198925	0	0		
	3:00	-12.476703	0	0		
	4:00	-12.682796	0	0		
	5:00	-12.951613	0	0		
	6:00	-13.189964	0	0		
	7:00	-13.430108	0	0		
	8:00	-13.591398	7.431546	0.3177		
	9:00	-13.738351	155.6166	6.65261		
	10:00	-13.842294	323.1123	13.8131		
	11:00	-13.394265	414.0985	17.7027	15	10.45
	12:00	-12.322581	459.0736	19.6254	15	10.45
	13:00	-11.148746	430.2477	18.3931	15	10.45
	14:00	-10.197133	428.0951	18.3011	15	10.45
	15:00	-9.4050179	345.4069	14.7661	10	9.05667
	16:00	-8.8691756	237.4085	10.1492		
	17:00	-8.6684588	73.94624	3.1612		
	18:00	-8.8333333	1.396402	0.0597		
	19:00	-9.4874552	0	0		
	20:00	-10.172043	0	0		
	21:00	-10.673835	0	0		
	22:00	-11.021505	0	0		
	23:00	-11.376344	0	0		
	0:00	-11.675627	0	0		
			718.9584	122.942		50.8567
July	1:00	15.6648746	0	0		
	2:00	15.3136201	0	0		
	3:00	14.9964158	0	0		
	4:00	14.6899642	0	0		
	5:00	14.4157706	11.80862	0.50482		
	6:00	14.2598566	139.8468	5.97845		
	7:00	15.2544803	290.2104	12.4065	10	12.54
	8:00	16.9032258	415.6348	17.7684	21	26.334
	9:00	18.390681	547.336	23.3986	32	40.128
	10:00	19.6792115	622.4744	26.6108	48	60.192
	11:00	20.7132616	613.1674	26.2129	53	66.462
	12:00	21.5824373	664.8648	28.423	53	66.462
	13:00	22.2526882	649.4443	27.7637	53	66.462
	14:00	22.8243728	656.9928	28.0864	53	66.462
	15:00	23.1218638	624.5609	26.7	53	66.462
	16:00	23.2329749	561.1409	23.9888	36	45.144
	17:00	23.0555556	487.8393	20.8551	25	31.35
	18:00	22.5555556	393.1755	16.8083	15	18.81
	19:00	21.8243728	209.5813	8.9596	12	15.048
	20:00	20.6577061	54.04109	2.31026		
	21:00	18.9086022	0	0		
	22:00	17.5304659	0	0		
	23:00	16.7688172	0	0		
	0:00	16.2240143	0	0		
			1735.53	296.776		581.856

February	1:00	-9.593254	0	0		
	2:00	-9.97619	0	0		
	3:00	-10.31349	0	0		
	4:00	-10.68849	0	0		
	5:00	-11.0119	0	0		
	6:00	-11.31944	0	0		
	7:00	-11.57937	0	0		
	8:00	-11.86508	79.9694	3.41869		
	9:00	-12.07143	271.114	11.5901		
	10:00	-11.88095	389.67	16.6584		
	11:00	-10.75595	502.397	21.4775	25	17.4167
	12:00	-9.353175	554.938	23.7236	22	19.9247
	13:00	-8.113095	555.58	23.751	22	19.9247
	14:00	-7.136905	544.577	23.2807	22	19.9247
	15:00	-6.33E+00	467.815	19.9991	20	18.1133
	16:00	-5.779762	377.081	16.1202	13	11.7737
	17:00	-5.482143	220.022	9.40596		
	18:00	-5.503968	46.5013	1.98793		
	19:00	-5.972222	0	0		
	20:00	-6.873016	0	0		
	21:00	-7.593254	0	0		
	22:00	-8.142857	0	0		
	23:00	-8.625	0	0		
	0:00	-9.051587	0	0		
			1002.42	171.413		107.078
August	1:00	15.22222	0	0		
	2:00	14.87276	0	0		
	3:00	14.55735	0	0		
	4:00	14.27778	0	0		
	5:00	14.06452	0	0		
	6:00	13.87276	51.3594	2.19561		
	7:00	14.15233	230.516	9.85456	10	12.54
	8:00	15.67384	374.88	16.0261	13	16.302
	9:00	17.22043	512.72	21.9188	32	40.128
	10:00	18.55735	586.234	25.0615	32	40.128
	11:00	19.70072	646.773	27.6495	48	60.192
	12:00	20.56452	630.877	26.97	53	66.462
	13:00	21.27419	646.313	27.6299	53	66.462
	14:00	21.85663	644.688	27.5604	53	66.462
	15:00	22.20251	614.961	26.2896	53	66.462
	16:00	22.26344	558.513	23.8764	36	45.144
	17:00	22.04659	429.633	18.3668	25	31.35
	18:00	21.50896	302.168	12.9177	15	18.81
	19:00	20.58423	121.207	5.18158		
	20:00	19.01613	6.18513	0.26441		
	21:00	17.39785	0	0		
	22:00	16.50717	0	0		
	23:00	15.97849	0	0		
	0:00	15.5448	0	0		
			1589.26	271.763		530.442

March	1:00	-4.3226	0	0		
	2:00	-4.7115	0	0		
	3:00	-5.0233	0	0		
	4:00	-5.3441	0	0		
	5:00	-5.6649	0	0		
	6:00	-5.9391	0	0		
	7:00	-6.181	49.609	2.12079		
	8:00	-6.1667	238.715	10.2051		
	9:00	-5.5771	401.072	17.1458	15	13.585
	10:00	-4.4892	527.845	22.5654	22	19.9247
	11:00	-3.2545	624.072	26.6791	35	31.6983
	12:00	-2.2204	676.102	28.9033	35	31.6983
	13:00	-1.3405	706.804	30.2159	54	48.906
	14:00	-0.6201	718.144	30.7007	54	48.906
	15:00	-0.0878	643.117	27.4932	35	31.6983
	16:00	0.20968	487.519	20.8414	15	18.81
	17:00	0.25627	382.468	16.3505	10	12.54
	18:00	4.15E-16	156.823	6.70418		
	19:00	-0.6129	10.3633	0.44303		
	20:00	-1.5323	0	0		
	21:00	-2.3047	0	0		
	22:00	-2.8781	0	0		
	23:00	-3.371	0	0		
	0:00	-3.7437	0	0		
			1405.66	240.368		257.767
Septemb	1:00	10.9815	0	0		
	2:00	10.6685	0	0		
	3:00	10.3574	0	0		
	4:00	10.1	0	0		
	5:00	9.8537	0	0		
	6:00	9.65556	4.66287	0.19934		
	7:00	9.52593	112.145	4.79419		
	8:00	10.3759	270.506	11.5641	10	12.54
	9:00	11.8537	385.262	16.4699	13	16.302
	10:00	13.2296	434.794	18.5875	21	26.334
	11:00	14.4074	522.767	22.3483	32	40.128
	12:00	15.3815	554.94	23.7237	32	40.128
	13:00	16.1907	556.344	23.7837	32	40.128
	14:00	16.7685	544.053	23.2583	32	40.128
	15:00	17.0722	480.052	20.5222	21	26.334
	16:00	17.0648	359.194	15.3555	13	16.302
	17:00	16.7315	295.016	12.6119	10	12.54
	18:00	15.9852	140.892	6.02313		
	19:00	14.6741	12.9958	0.55557		
	20:00	13.1148	0	0		
	21:00	12.2815	0	0		
	22:00	11.763	0	0		
	23:00	11.4167	0	0		
	0:00	11.0611	0	0		
			1168.41	199.797		270.864

April	1:00	2.02407	0	0		
	2:00	1.65185	0	0		
	3:00	1.36111	0	0		
	4:00	1.06852	0	0		
	5:00	0.78148	0	0		
	6:00	0.55	46.8747	2.0039		
	7:00	0.6	222.941	9.53073		
	8:00	1.79815	385.383	16.4751	13	16.302
	9:00	3.29074	570.063	24.3702	28	35.112
	10:00	4.57963	638.705	27.3047	43	53.922
	11:00	5.68519	705.202	30.1474	61	76.494
	12:00	6.58704	755.601	32.3019	61	76.494
	13:00	7.29815	748.432	31.9955	61	76.494
	14:00	7.87222	733.436	31.3544	61	76.494
	15:00	8.17963	670.759	28.675	43	53.922
	16:00	8.28519	574.701	24.5685	28	35.112
	17:00	8.09815	429.523	18.3621	20	25.08
	18:00	7.60926	293.516	12.5478		
	19:00	6.74074	98.9494	4.23009		
	20:00	5.44074	1.03855	0.0444		
	21:00	4.40556	0	0		
	22:00	3.63148	0	0		
	23:00	3.07037	0	0		
	0:00	2.62222	0	0		
			1718.78	293.912		525.426
October	1:00	4.77957	0	0		
	2:00	4.50538	0	0		
	3:00	4.26882	0	0		
	4:00	4.06093	0	0		
	5:00	3.85484	0	0		
	6:00	3.61111	0	0		
	7:00	3.49104	34.3533	1.4686		
	8:00	3.55735	217.934	9.31668	10	12.54
	9:00	4.59677	386.164	16.5085	13	16.302
	10:00	5.88351	496.278	21.2159	20	25.08
	11:00	6.99821	499.175	21.3397	20	25.08
	12:00	7.92473	543.594	23.2387	28	35.112
	13:00	8.69534	539.815	23.0771	28	35.112
	14:00	9.29211	484.18	20.6987	20	25.08
	15:00	9.57348	414.237	17.7086	20	25.08
	16:00	9.53226	342.068	14.6234	13	16.302
	17:00	9.0914	195.949	8.37684		
	18:00	8.16846	22.1076	0.9451		
	19:00	6.98208	0	0		
	20:00	6.2509	0	0		
	21:00	5.76523	0	0		
	22:00	5.4086	0	0		
	23:00	5.14516	0	0		
	0:00	4.88172	0	0		
			1043.96	178.518		215.688

May	1:00	7.82258	0	0		
	2:00	7.39964	0	0		
	3:00	7.05556	0	0		
	4:00	6.75269	0	0		
	5:00	6.4319	11.273	0.48192		
	6:00	6.2491	114.405	4.89082		
	7:00	7.19534	272.398	11.645	10	12.54
	8:00	8.84229	410.105	17.532	20	25.08
	9:00	10.31	508.766	21.7497	32	40.128
	10:00	11.5108	567.906	24.278	32	40.128
	11:00	12.5556	581.616	24.8641	32	40.128
	12:00	13.4695	655.569	28.0256	48	60.192
	13:00	14.1237	617.034	26.3782	48	60.192
	14:00	14.6971	606.037	25.9081	48	60.192
	15:00	15.0287	534.258	22.8395	32	40.128
	16:00	15.0986	504.74	21.5777	32	40.128
	17:00	14.8387	434.043	18.5553	21	26.334
	18:00	14.3297	316.505	13.5306	13	16.302
	19:00	13.5591	160.718	6.8707		
	20:00	12.3513	24.4439	1.04498		
	21:00	10.8871	0	0		
	22:00	9.76882	0	0		
	23:00	9.01434	0	0		
	0:00	8.44982	0	0		
			1579.95	270.172		461.472
Novembe	1:00	-2.2519	0	0		
	2:00	-2.4741	0	0		
	3:00	-2.6556	0	0		
	4:00	-2.7889	0	0		
	5:00	-2.9611	0	0		
	6:00	-3.1407	0	0		
	7:00	-3.2926	0	0		
	8:00	-3.4667	62.2902	2.66291		
	9:00	-3.2148	207.299	8.86203		
	10:00	-2.3574	333.463	14.2556	10	9.05667
	11:00	-1.4722	380.238	16.2552	10	9.05667
	12:00	-0.6315	400.858	17.1367	15	13.585
	13:00	0.07037	410.202	17.5361	20	25.08
	14:00	0.6037	373.886	15.9836	13	16.302
	15:00	0.88889	283.049	12.1004	10	12.54
	16:00	0.85741	174.42	7.45645		
	17:00	0.4	39.9421	1.70753		
	18:00	-0.5093	0	0		
	19:00	-1.0574	0	0		
	20:00	-1.45	0	0		
	21:00	-1.7111	0	0		
	22:00	-1.9537	0	0		
	23:00	-2.163	0	0		
	0:00	-2.3537	0	0		
			666.412	113.956		85.6203

June	1:00	12.6333	0	0		
	2:00	12.2	0	0		
	3:00	11.8426	0	0		
	4:00	11.5796	0	0		
	5:00	11.3	20.6429	0.88248		
	6:00	11.3241	130.128	5.56297		
	7:00	12.5556	243.405	10.4055	10	12.54
	8:00	14.1222	362.833	15.5111	13	16.302
	9:00	15.5296	445.386	19.0402	21	26.334
	10:00	16.687	531.026	22.7014	32	40.128
	11:00	17.6833	558.192	23.8627	32	40.128
	12:00	18.5056	548.117	23.432	32	40.128
	13:00	19.1278	516.642	22.0864	32	40.128
	14:00	19.6426	465.598	19.9043	21	26.334
	15:00	19.9481	414.129	17.704	21	26.334
	16:00	20.0056	414.667	17.727	25	31.35
	17:00	19.8093	358.359	15.3199	13	16.302
	18:00	19.3815	252.96	10.814	10	12.54
	19:00	18.7056	132.971	5.68452		
	20:00	17.5796	40.8173	1.74494		
	21:00	15.9944	0	0		
	22:00	14.6037	0	0		
	23:00	13.7944	0	0		
	0:00	13.2667	0	0		
			1358.97	232.384		328.548
Decembe	1:00	-9.7545	0	0		
	2:00	-9.9659	0	0		
	3:00	-10.14	0	0		
	4:00	-10.337	0	0		
	5:00	-10.471	0	0		
	6:00	-10.613	0	0		
	7:00	-10.733	0	0		
	8:00	-10.88	8.57053	0.36639		
	9:00	-10.941	102.276	4.37232		
	10:00	-10.466	228.185	9.7549		
	11:00	-9.5251	333.099	14.24	10	9.05667
	12:00	-8.5735	349.882	14.9574	10	9.05667
	13:00	-7.7849	356.333	15.2333	10	9.05667
	14:00	-7.147	321.375	13.7388	10	9.05667
	15:00	-6.7688	230.648	9.86022		
	16:00	-6.7204	132.084	5.64659		
	17:00	-7.1111	20.3504	0.86998		
	18:00	-7.8208	0	0		
	19:00	-8.2867	0	0		
	20:00	-8.6129	0	0		
	21:00	-8.8799	0	0		
	22:00	-9.1774	0	0		
	23:00	-9.4301	0	0		
	0:00	-9.6846	0	0		
			520.701	89.0399		36.2267